



Original article

Exploring the 7-oxo-thiazolo[5,4-d]pyrimidine core for the design of new human adenosine A₃ receptor antagonists. Synthesis, molecular modeling studies and pharmacological evaluation



Flavia Varano ^{a,*}, Daniela Catarzi ^a, Lucia Squarcialupi ^a, Marco Betti ^a, Fabrizio Vincenzi ^b, Annalisa Ravani ^b, Katia Varani ^b, Diego Dal Ben ^c, Ajiroghene Thomas ^c, Rosaria Volpini ^c, Vittoria Colotta ^a

^a Dipartimento di Neuroscienze, Psicologia, Area del Farmaco e Salute del Bambino, Sezione di Farmaceutica e Nutraceutica, Università di Firenze, Polo Scientifico, Via Ugo Schiff 6, 50019 Sesto Fiorentino, FI, Italy

^b Dipartimento di Medicina Clinica e Sperimentale, Sezione di Farmacologia, Università di Ferrara, Via Fossato di Mortara 17-19, 44121 Ferrara, Italy

^c School of Pharmacy, Medicinal Chemistry Unit, University of Camerino, Via S. Agostino 1, 62032 Camerino, MC, Italy

ARTICLE INFO

Article history:

Received 1 December 2014

Received in revised form

31 March 2015

Accepted 3 April 2015

Available online 4 April 2015

Keywords:

G protein-coupled receptors

Adenosine receptor antagonists

Thiazolopyrimidine

Bicyclic heteroaromatic systems

Ligand-receptor modeling studies

ABSTRACT

A new series of 5-methyl-thiazolo[5,4-d]pyrimidine-7-ones bearing different substituents at position 2 (aryl, heteroaryl and arylamino groups) was synthesized and evaluated in radioligand binding assays to determine their affinities at the human (h) A₁, A_{2A}, and A₃ adenosine receptors (ARs). Efficacy at the hA_{2B} and antagonism of selected ligands at the hA₃ were also assessed through cAMP experiments. Some of the new derivatives exhibited good to high hA₃AR affinity and selectivity versus all the other AR subtypes. Compound 2-(4-chlorophenyl)-5-methyl-thiazolo[5,4-d]pyrimidine-7-one **4** was found to be the most potent and selective ligand of the series (*K_i*; hA₃ = 18 nM). Molecular docking studies of the reported derivatives were carried out to depict their hypothetical binding mode in our hA₃ receptor model.

© 2015 Elsevier Masson SAS. All rights reserved.

1. Introduction

Purine nucleoside adenosine regulates a large number of pathophysiological processes through activation of four known receptor subtypes (A₁, A_{2A}, A_{2B} and A₃) which are cell surface G protein-coupled receptors [1,2]. Activation of adenosine receptors (ARs) typically inhibits (A₁ and A₃) or stimulates (A_{2A} and A_{2B}) adenylyl cyclase, but other second messengers can be modulates the most important being inositol trisphosphate (IP₃) and diacylglycerol (DAG). Therefore, adenosine receptors (ARs) are valid targets for the development of new therapeutic agents

in several pathological conditions. Selective modulation of each receptor subtype has been recognized as therapeutically useful in many disorders such as cerebral ischemia, asthma, renal failure, CNS disorders, inflammatory and neurodegenerative diseases [1–6].

Among the ARs, the A₃AR is the latest to be cloned and pharmacologically characterized, consequently its role in several therapeutic fields, including ischemia, inflammation and cancer, is still controversial. In particular, antagonists of the A₃AR have been shown to be attractive as novel potential anti-inflammatory drugs as well as for the treatment of glaucoma and in cancer chemotherapy [7–11]. Moreover, in the CNS, the A₃AR is expressed in neurons and glial cells which are recognized as structural supports for neurons and as active participants in various neurodegenerative diseases [12–14].

The putative therapeutic applications of human (h) A₃AR antagonists as well as the growing need of pharmacological tools to clarify the A₃ AR roles has made the search for new potent and selective hA₃AR antagonists an emerging and stimulating medicinal chemistry topic [7].

Abbreviations: MRS 1220, 9-Chloro-2-(2-furanyl)-5-((phenylacetyl)amino)-[1,2,4]triazolo[1,5-c]quinazoline; NECA, 5'-N-ethyl-carboxamidoadenosine; cAMP, cyclic adenosine monophosphate; DPCPX, 8-cyclopentyl-1,3-dipropyl-xanthine; ZM-241385, 4-(2-[7-amino-2-(2-furyl)]1,2,4-triazolo[2,3-a][1,3,5]triazin-5-ylamino)ethylphenol; 1-AB-MECA, N⁶-(4-amino-3-iodobenzyl)-5'-N-methylcarboxamido adenosine.

* Corresponding author.

E-mail address: flavia.varano@unifi.it (F. Varano).

In our laboratory we have also devoted much effort to the study of AR antagonists belonging to different heterocyclic classes, and have identified many potent hA₃AR antagonists [15–30]. Recently, we disclosed a class of bicyclic hA₃AR antagonists, the 2-arylpyrazolo[4,3-d]pyrimidin-7-one (PP) derivatives endowed with high hA₃AR affinity ($K_i = 1.2\text{--}72$ nM) and selectivity (Fig. 1) [23]. Molecular modeling studies indicated that PP derivatives are anchored at the binding site through two stabilizing hydrogen-bonding interactions that involve, as hydrogen accepting groups, the 7-oxo function and the nitrogen atom at position-1 [23].

Therefore, to develop a new class of compounds targeting the ARs, we design the thiazolo[5,4-d]pyrimidine-7-one (TP) derivatives **1–33** (Fig. 2). The thiazolo pyrimidine core maintains a size and shape similar to the pyrazolo pyrimidine nucleus, as well as the structural features (the 7-oxo function and the nitrogen atom at position-1) able to engage the above mentioned crucial interactions with the receptor site.

Structure–affinity relationship (SAR) analysis of PP derivatives allowed us to deduce other structural features that could be important for the hA₃AR receptor–ligand interaction. In particular, the presence of a small lipophilic substituent, such as a methyl or an ethyl group, at the 5-position of the PP scaffold, significantly enhances the hA₃AR binding affinity of the ligands, probably because these groups engage hydrophobic bonds with a lipophilic receptor pocket of limited size [23]. Hence, the 5-position of all the newly synthesized TP derivatives (compounds **1–33**) was functionalized with a methyl group.

In addition, the TP derivatives were obtained following chemical synthetic procedures much more easier than those used for the synthesis of compounds PP. This feature has made it possible to synthesize several compounds that differ in the nature of the substituent at position-2 of the TP core and, thus, has made it possible to deeply investigate the interaction between the substituent at that position and the receptor cleft that receives it.

In the PP lead series, the presence of a 4-methoxy or a 4-methyl group on the 2-phenyl ring was found to increase hA₃AR affinity [23]. Therefore, in the new series, these substituents and others with different electronic and steric properties (Cl, F, CF₃, COOH, OH) were probed at para- and meta-positions of the 2-phenyl ring (compounds **1–13**).

Moreover, further groups were introduced at position-2 of the TP nucleus: i.e. heterocyclic substituents (compounds **15–20**), and a benzyl (compound **14**) or arylamino chain (compounds **21–28**), to space the phenyl moiety from the bicyclic thiazolo pyrimidine core.

Finally, in some selected 2-aryl- and 2-arylamino-substituted compounds, the hydrogen accepting 7-oxo group was replaced by a 7-ethoxy function (compounds **29–31** and **32–33**, respectively) which shows the same capability of engaging a hydrogen bond but is more cluttered than the corresponding 7-oxo moiety.

The new derivatives (**1–33**) were tested to evaluate their affinities at hA₁, hA_{2A} and hA₃ARs and their efficacy at hA_{2B}AR. Two selected compounds, i.e. the 2-phenyl-thiazolopyrimidine-7-one **1** and the 2-(4-chlorophenyl)-thiazolopyrimidine-7-one **4**, were also

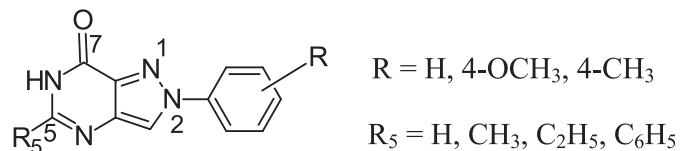


Fig. 1. Previously reported 2-arylpyrazolo[4,3-d]pyrimidin-7-one derivatives (Series PP).

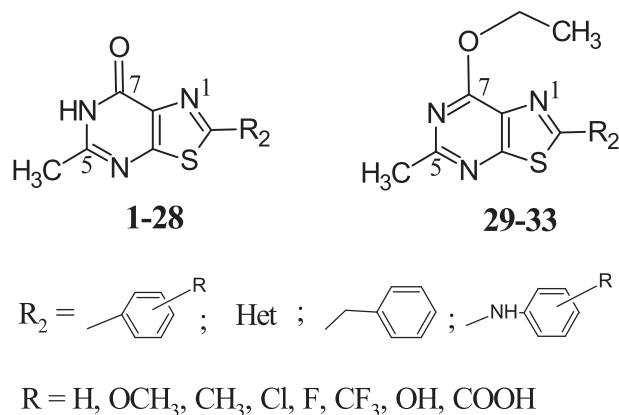


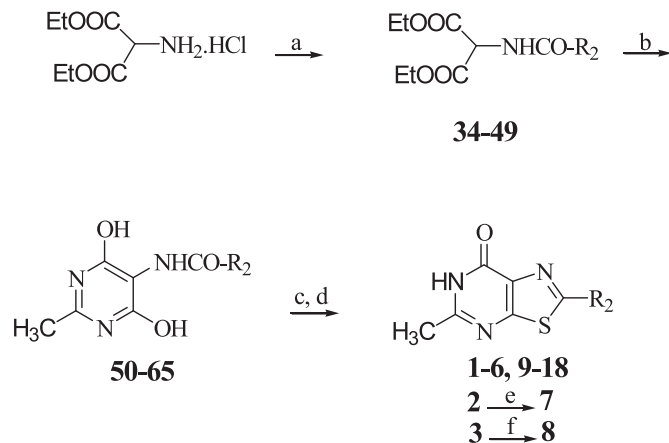
Fig. 2. Herein reported thiazolo[5,4-d]pyrimidine (Series TP).

analyzed to assess their hA₃ antagonistic activity.

Along with the pharmacological evaluation, we carried out molecular modeling studies of the new derivatives to better rationalize the available SARs.

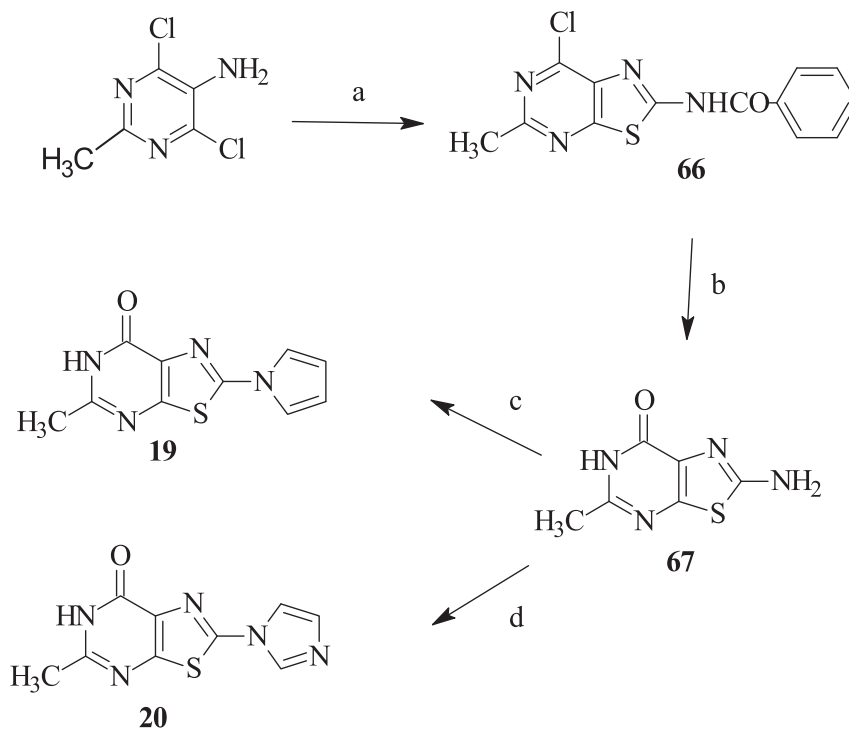
2. Chemistry

Compounds **1–33** were synthesized as depicted in Schemes 1–5. Briefly, the 2-aryl derivatives **1–13**, the 2-benzyl substituted **14** and the 2-heteroaryl thiazolopyrimidines **15–18**, were obtained starting from the commercially available 2-amino malonate hydrochloride which was reacted with suitable acyl chlorides to yield the amides **34–49** (Scheme 1) [31–37]. Most of the acyl chlorides



	R ₂		R ₂
34, 50, 1	C ₆ H ₅	41, 57, 10	3-CH ₃ -C ₆ H ₄
35, 51, 2	4-OCH ₃ -C ₆ H ₄	42, 58, 11	3-Cl-C ₆ H ₄
36, 52, 3	4-CH ₃ -C ₆ H ₄	43, 59, 12	3-F-C ₆ H ₄
37, 53, 4	4-Cl-C ₆ H ₄	44, 60, 13	3-CF ₃ -C ₆ H ₄
38, 54, 5	4-F-C ₆ H ₄	45, 61, 14	CH ₂ -C ₆ H ₅
39, 55, 6	4-CF ₃ -C ₆ H ₄	46, 62, 15	3-pyridyl
7	4-OH-C ₆ H ₄	47, 63, 16	4-pyridyl
8	4-COOH-C ₆ H ₄	48, 64, 17	2-furyl
40, 56, 9	3-OCH ₃ -C ₆ H ₄	49, 65, 18	2-thienyl

Scheme 1. Reagents and conditions: a) for **34, 35, 46, 47**: R₂COCl, Py, room temperature, for **36–45, 48–49**: R₂COCl, NaHCO₃, Et₂O/H₂O, 0 °C; b) acetamide hydrochloride, NaOEt, EtOH, reflux; c) i) P₂S₅, Py, reflux; ii) conc HCl, NMP, reflux; d) 1.5 M NaOH, H₂O₂, H₂O, room temperature; e) BBr₃, CH₂Cl₂ reflux; f) CrO₃, conc H₂SO₄, H₂O, room temperature.



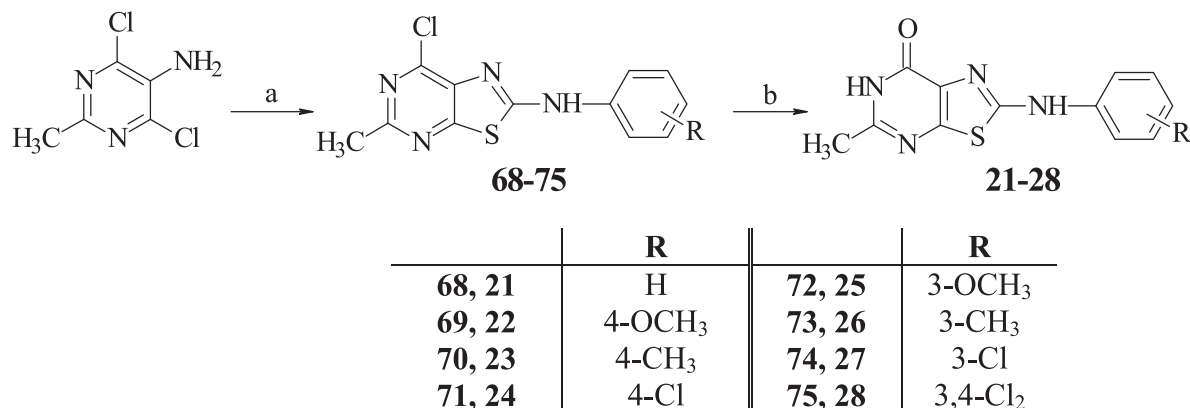
Scheme 2. Reagents and conditions: a) benzoylisothiocyanate, acetone, reflux; b) 6 M HCl, reflux; c) 2,5-diethoxytetrahydrofuran, acetic acid, 90 °C; d) 37% aqueous formaldehyde, 40% aqueous glyoxal, ammonium acetate, acetic acid, 70 °C.

were commercial except the nicotinoyl and isonicotinoyl chlorides which were synthesized following literature procedures [38,39]. Allowing the amides **34–49** to react with an excess of acetamidine hydrochloride in the presence of sodium ethoxide, the corresponding 4,6-dihydroxy-2-methyl-pyrimidine-5-amido derivatives **50–65** were isolated [40]. By refluxing the latter in pyridine with P_2S_5 and, successively, by treating the mixture with concentrated HCl in *N*-methyl-2-pyrrolidone and successively with hydrogen peroxide at room temperature, the corresponding 7-oxo-thiazolo[5,4-*d*]pyrimidine derivatives **1–6**, **9–18** were obtained [40]. Demethylation with BBr_3 of the 2-(4-methoxy-phenyl) derivative **2** afforded the 2-(4-hydroxyphenyl) substituted **7**. Otherwise, oxidation with CrO_3 of 2-(4-methyl-phenyl) derivative **3** yielded the corresponding 2-(4-carboxyphenyl) compound **8**.

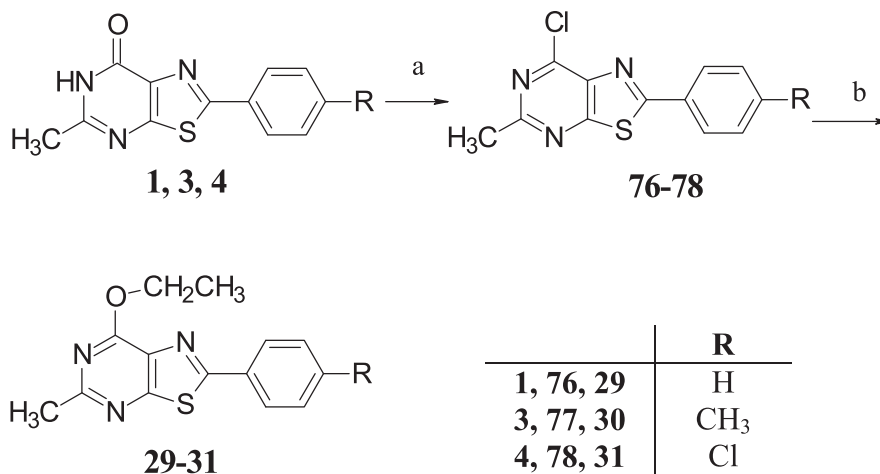
For the synthesis of the 2-heteroaryl-thiazolopyrimidines **19–20** another procedure involving the 5-methyl-7-oxo-thiazolo

[5,4-*d*]pyrimidine-2-amino derivative **67** as key intermediate was followed (Scheme 2). **67** was synthesized by reaction of the commercial 5-amino-4,6-dichloro-2-methylpyrimidine with benzoylisothiocyanate and subsequent acid-catalyzed hydrolysis of the obtained 7-chloro-2-benzoylamino-thiazolo[5,4-*d*]pyrimidine **66**. By reacting the intermediate 2-amino-thiazolopyrimidine **67** either with 2,5-diethoxytetrahydrofuran, or formaldehyde glyoxale and ammonium acetate, in acetic acid, the 2-(pyrrol-1-yl)- and the 2-(imidazol-1-yl)- **19** and **20**, respectively, were obtained.

Scheme 3 shows the synthesis of the thiazolopyrimidine-2-arylamino derivatives **21–28**. Allowing the commercially available 5-amino-4,6-dichloro-2-methylpyrimidine to react with suitable arylisothiocyanate in the presence of cesium carbonate, the corresponding 7-chloro-5-methyl-*N*-(aryl)-thiazolo[5,4-*d*]pyrimidin-2-amines **68–75** were obtained, which were treated with sodium acetate and acetic acid to afford the corresponding 7-oxo-



Scheme 3. Reagents and conditions: a) arylisothiocyanate, Cs_2CO_3 , acetonitrile, 50 °C; b) CH_3COONa , acetic acid, mw or conventional heating 140 °C.



Scheme 4. Reagents and conditions: a) POCl₃, N,N-dimethylaniline, reflux; b) DBU, abs EtOH, mw 160 °C.

thiazolopyrimidine-2-arylamino derivatives **21–28**.

The 7-ethoxy-thiazolopyrimidine derivatives **29–31** and **32–33** were obtained as reported in [Schemes 4 and 5](#), respectively. By reaction with POCl₃, the 7-oxo-2-aryl-thiazolopyrimidines **1, 3, 4** were transformed into the corresponding 7-chloro-2-aryl-thiazolopyrimidine derivatives **76–78** [41] which were microwave irradiated at 160 °C in the presence of ethanol and 1,8-diazabicyclo [5.4.0]undec-7-ene (DBU) to give the 7-ethoxy derivatives **29–31** ([Scheme 4](#)). Finally, the 7-chloro-2-arylamino derivatives **68** and **72** were treated respectively with an aqueous solution of NaOH or EtONa in absolute ethanol to afford the corresponding 7 ethoxy-2-arylamino **32** and **33** ([Scheme 5](#)).

3. Pharmacology

All the newly synthesized compounds (**1–33**) were evaluated in radioligand binding assays to determine their affinities for hA₁, hA_{2A} and hA₃ARs expressed in CHO cells. In particular [³H]DPCPX [³H]ZM-241385 and [¹²⁵I]AB-MECA were used as radioligands to hA₁, hA_{2A} and hA₃ARs, respectively. The efficacy of the compounds to hA_{2B}AR was investigated by evaluating their capability to inhibit (100 nM) NECA-stimulated adenylyl cyclase activity.

Antagonism of selected ligands, i.e. the 2-phenyl-thiazolo[5,4-d]pyrimidin-7-one **1** and the 2-(4-chlorophenyl)-thiazolo[5,4-d]pyrimidin-7-one **4**, at hA₃AR was also assessed through cAMP experiments, by evaluating their capability to block the inhibition of cAMP production mediated by Cl-IB-MECA (100 nM).

Affinity data for hA₁, hA_{2A} and hA₃ARs (expressed as K_i values or I%), and IC₅₀ values or I% for hA_{2B} and hA₃AR, derived from the cAMP assays, of compounds **1–33** along with the previously

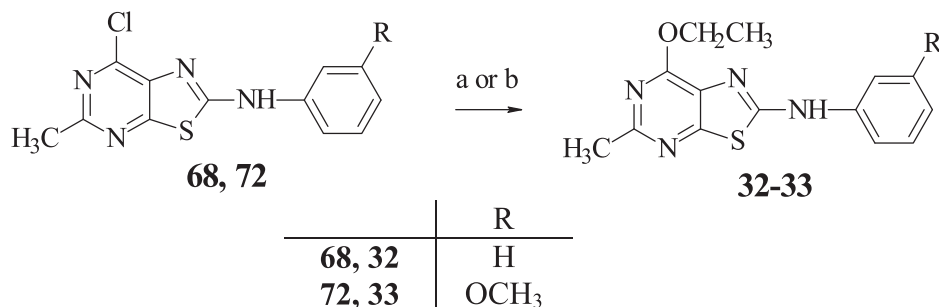
reported **PP-1A** as reference, are listed in [Table 1](#).

4. Results and discussion

4.1. Structure–affinity relationship studies

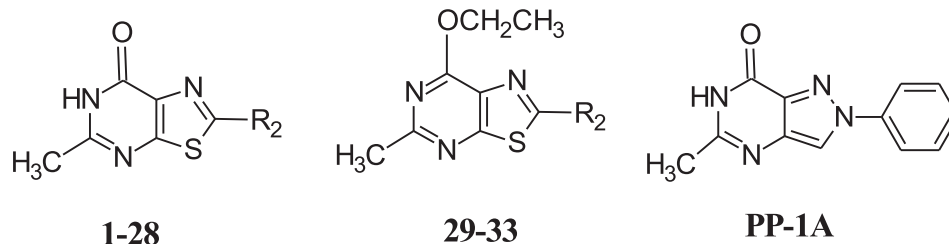
As clearly shown in [Table 1](#), some of the synthesized compounds (**1–33**) possess good hA₃AR affinity and high selectivity being almost inactive at all the other ARs. These data are very encouraging and suggest that the thiazolo[5,4-d]pyrimidine ring system can be considered as a new scaffold for the development of potent and selective hA₃AR antagonists. In fact, the 2-phenyl parent **1** (K_i = 85 nM) displays an hA₃AR binding affinity value only 5-fold lower than the corresponding **PP-1A** derivative.

It is quite evident ([Table 1](#)) that the highest hA₃AR binding affinity is attributable to the thiazolo pyrimidine derivatives bearing a 7-oxo moiety and an aryl group at position-2 (compounds **1–13**). In particular, the 7-oxo-2-(4-chlorophenyl)- derivative **4** emerges as the most interesting compound, showing a nanomolar hA₃AR affinity (K_i = 18 nM) which is 5-fold higher than that of the parent **1**. The introduction of groups with different electronic and lipophilic properties in para- or meta-position on the appended 2-phenyl ring of **1**, differently affects the affinity at the hA₃AR. In particular, as already observed for the 4-chloro substituent (see compound **4**), the presence of a lipophilic 4-methoxy or 4-methyl group, seems to positively affect hA₃AR affinity. Indeed, the 2-(4-methoxyphenyl)-**2** and the 2-(4-methylphenyl)-**3** display comparable binding affinity that is higher than that of the 2-phenyl unsubstituted **1**. In contrast, the presence of the hydrophobic 4-trifluoromethyl group exerts a deleterious effect on hA₃AR binding affinity (compare **6**



Scheme 5. Reagents and conditions: a) 20% aqueous NaOH, EtOH, reflux; b) EtONa, EtOH, reflux.

Table 1
Binding Affinity (K_i) at hA₁, hA_{2A}, and hA₃ARs and Potencies (IC₅₀) at hA_{2B} and hA₃ARs.



Comp	R ₂	Binding experiments ^a K _i (nM) or I %			cAMP assays IC ₅₀ (nM) or I%	
		hA ₁ ^b	hA _{2A} ^c	hA ₃ ^d	hA _{2B} ^e	hA ₃ ^f
1	C ₆ H ₅	11%	1%	85 ± 9	1%	221 ± 24
2	4-OCH ₃ -C ₆ H ₄	10%	1%	38 ± 4	3%	
3	4-CH ₃ -C ₆ H ₄	17%	2%	33 ± 4	3%	
4	4-Cl-C ₆ H ₄	1%	1%	18 ± 2	1%	42 ± 4
5	4-F-C ₆ H ₄	1%	15%	107 ± 9	17%	
6	4-CF ₃ -C ₆ H ₄	1%	37%	32%	1%	
7	4-OH-C ₆ H ₄	1%	1%	15%	1%	
8	4-COOH-C ₆ H ₄	1%	1%	1%	1%	
9	3-OCH ₃ -C ₆ H ₄	1%	12%	28%	4%	
10	3-CH ₃ -C ₆ H ₄	1%	31%	384 ± 36	1%	
11	3-Cl-C ₆ H ₄	24%	10%	826 ± 79	1%	
12	3-F-C ₆ H ₄	1%	1%	109 ± 11	1%	
13	3-CF ₃ -C ₆ H ₄	1%	15%	15%	17%	
14	CH ₂ -C ₆ H ₅	11%	1%	427 ± 46	1%	
15	3-pyridyl	1%	1%	33%	1%	
16	4-pyridyl	1%	1%	15%	1%	
17	2-furyl	37%	1%	20%	2%	
18	2-thienyl	4%	1%	248 ± 21	1%	
19	pyrrol-1-yl	1%	9%	227 ± 19	3%	
20	imidazol-1-yl	1%	1%	8%	1%	
21	NH-C ₆ H ₅	24%	14%	45%	1%	
22	NH-(4-OCH ₃ -C ₆ H ₄)	1%	1%	36%	1%	
23	NH-(4-CH ₃ -C ₆ H ₄)	20%	18%	47%	1%	
24	NH-(4-Cl-C ₆ H ₄)	33%	18%	49%	1%	
25	NH-(3-OCH ₃ -C ₆ H ₄)	8%	1%	113 ± 10	1%	
26	NH-(3-CH ₃ -C ₆ H ₄)	12%	8%	450 ± 42	1%	
27	NH-(3-Cl-C ₆ H ₄)	44%	21%	48%	1%	
28	NH-(3,4-Cl ₂ -C ₆ H ₃)	30%	16%	25%	1%	
29	C ₆ H ₅	11%	1%	6%	1%	
30	4-CH ₃ -C ₆ H ₄	1%	1%	5%	1%	
31	4-Cl-C ₆ H ₄	6%	9%	10%	1%	
32	NH-C ₆ H ₅	2%	3%	45%	1%	
33	NH-(3-OCH ₃ -C ₆ H ₄)	3%	25%	110 ± 12	1%	
PP-1A^g	—	1%	1%	16 ± 2	2%	

^a K_i values are means ± SEM of four separate assays each performed in duplicate. Percentage of inhibition (I %) is determined at 1 μM concentration of the tested compounds.

^b Displacement of specific [³H]DPCPX competition binding assays to hA₁CHO cells.

^c Displacement of specific [³H]ZM241385 competition binding to hA_{2A}CHO cells.

^d Displacement of specific [¹²⁵I]AB-MECA competition binding to hA₃CHO cells.

^e cAMP experiments in hA_{2B}CHO cells, stimulated by 200 nM NECA. Percentage of inhibition (I%) is determined at 1 μM concentration of the tested compounds.

^f IC₅₀ values are expressed as means ± SEM of four separate cAMP experiments in hA₃CHO cells, in the presence of 100 nM CI-IB-MECA.

^g Ref. [23].

with **1**). The 2-(4-fluorophenyl) substituted compound **5** does not show any appreciable difference in the hA₃ AR affinity with respect to the 2-phenyl derivative **1**. Finally, introduction of a hydrophilic 4-hydroxyl or 4-carboxy substituent turns out to be detrimental for hA₃AR affinity (compare **7**, **8** with **1**). It is interesting to point out that the movement of the methoxy, methyl or chloro group, from the para-to the meta-position, results in an important drop of the hA₃ affinity (compare **9**, **10**, **11**, to **2**, **3**, **4** respectively). On the contrary, the same shift of the fluorine substituent does not affect the hA₃AR binding affinity (compare **12** to **5**, respectively).

Replacement of the 2-phenyl ring of **1** with different heterocyclic residues (compounds **15**–**20**) leads to results which are difficult to explain. In fact, a comparison of the hA₃ affinity value of the 2-

phenyl derivative **1** with those of the 2-(2-thienyl)- **18** and the 2-(pyrrol-1-yl)- substituted **19**, indicates a substantial bioisosterism of these substituents as regards the interaction with the hA₃ receptor site, even if the 2-heterocyclic substituted compounds **18** and **19** are about 3-fold less active than the 2-phenyl derivative **1**. On the contrary, replacement of the phenyl ring with a 2-(3-pyridyl)- (**15**), a 2-(4-pyridyl)- (**16**), a 2-(2-furyl)- (**17**) or with a 2-(imidazol-1-yl)- (**20**) leads to a substantial loss of hA₃AR affinity.

Continuing to investigate the SARs of these new hA₃AR ligands, we decided to distance the 2-phenyl moiety of compound **1** from the bicyclic core via a methylene (compound **14**) or an amino (compound **21**) linker. In both cases, the hA₃ receptor binding is maintained but the affinity decreases. Thus, with the aim of

improving hA₃AR binding activity of the 2-phenylamino substituted compound **21**, we inserted on the appended 2-phenyl ring those substituents that in the 2-aryl series afforded the highest hA₃AR binding affinity. Thus, we introduced a methoxy, a methyl group or a chlorine atom either in para- (**22–24**) or meta-position (**25–27**) on the appended phenylamino chain. Overall, these substituents do not exert the desired effect observed in the 2-aryl substituted series (**1–13**). The only exceptions are the 3-methoxy and 3-methyl groups that make compounds **25** and **26**, respectively, more active than the unsubstituted parent compound **21**, while a chlorine atom in the same position does not affect hA₃ binding.

Differences between the SARs of the 2-aryl and the 2-aryl-amino substituted compounds are also evidenced by the different binding behavior of the 7-ethoxy derivatives of the two series **29–31** and **32–33**. In fact, in the 2-aryl-7-ethoxy derivatives **29–31** we observe a dramatic drop of the hA₃AR binding activity compared to their corresponding 7-oxo compounds **1, 3–4**. In contrast, the 2-aryl-amino-7-ethoxy **32** and **33** and their corresponding 7-oxo- **21** and **25** bind to the hA₃AR with similar affinities.

The selected compounds **1** and **4** were tested to evaluate their antagonistic potencies to modulate CI-IB-MECA inhibited cAMP accumulation in CHO cells expressing the hA₃ receptor. In accordance with the hA₃AR affinity values, the IC₅₀ results (Table 1) showed that the tested compounds are hA₃AR antagonists endowed with significant potencies.

4.2. Molecular modeling studies

A molecular docking analysis was performed on a homology model of hA₃AR developed by using the X-ray structure of the hA_{2A}AR as template (pdb code: 3EML; 2.6 Å resolution [42]). This crystal structure has been solved in complex with a high affinity antagonist (ZM241385), hence presenting an inactive conformation and a cavity suitable as a binding site for docking analysis [43]. The sequence alignment of the four human ARs is shown within Supplementary data. The obtained hA₃AR homology model was checked by using the Protein Geometry Monitor application within MOE [44], which provides a variety of stereochemical measurements for inspection of the structural quality in a given protein, such as backbone bond lengths, angles and dihedrals, Ramachandran ϕ - ψ dihedral plots, and sidechain rotamer and nonbonded contact quality.

A preliminary docking analysis was performed by manually docking the high affinity antagonist MRS 1220 (K_i hA₃AR = 0.65 nM [45]) structure within the hA₃AR model binding site. The obtained hA₃AR-MRS 1220 complex was then subjected to energy minimization refinement and to Monte Carlo analysis (with Schrodinger Macromodel [46] software) to explore the favorable binding conformations, with the input structure consisting of the ligand and a shell of receptor amino acids within 6 Å distance from it. The coordinates of the remaining receptor residues were kept fixed. During the Monte Carlo conformational search (10,000 steps), the input structure was modified by random changes in torsion angles (for all input structure residues), and molecular position (for the ligand). Hence, the ligand was left free to be continuously re-oriented and re-positioned within the binding site and the conformation of both ligand and internal shell residues could be explored and reciprocally relaxed. This stage allowed us to provide an hA₃AR binding site conformation able to accommodate the analyzed antagonists. The best receptor-MRS 1220 complex was subjected to energy minimization. The RMSD value (calculated within MOE; only backbone atoms were considered) from the comparison of the initial and the final model was 0.32 Å. This value raises to 0.53 Å considering only the receptor residues subjected to

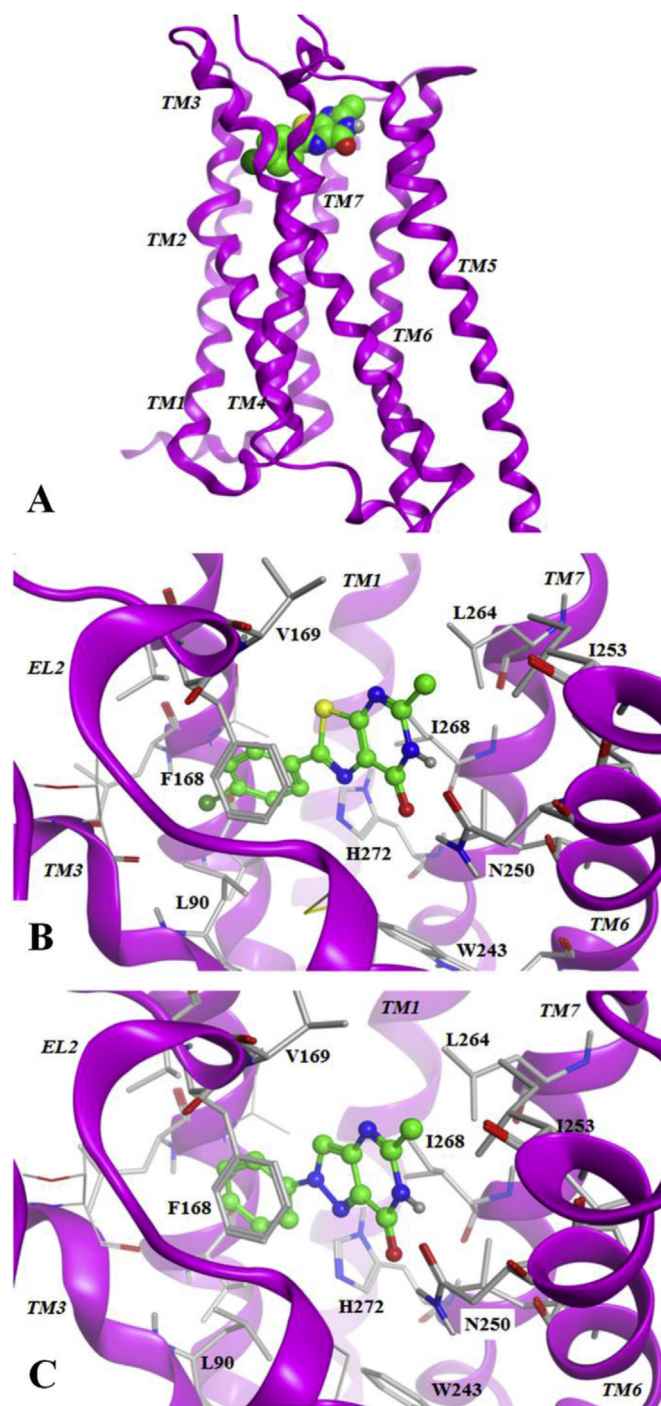


Fig. 3. A. Side view of the hA₃AR model with indication of the compounds binding mode (compound **4** is shown). B. Detailed view of the binding mode of the synthesised compounds. The compound **4** is shown. The picture displays, in particular, the interaction of the scaffold with the receptor residues. The double H-bond interaction of the compound scaffold with the sidechain of Asn250 is clearly visible. C. Detailed view of the binding mode of the compound PP-1A.

Monte Carlo conformational search.

Once the MRS 1220 compound was removed, the hA₃AR model was then used as a target for the docking analysis of the synthesized derivatives. All ligand structures were optimized using RHF/AM1 semi-empirical calculations (with the software package MOPAC [47] implemented in MOE) and then docked into the binding site of the hA₃AR model by using the MOE Dock tool. Top-

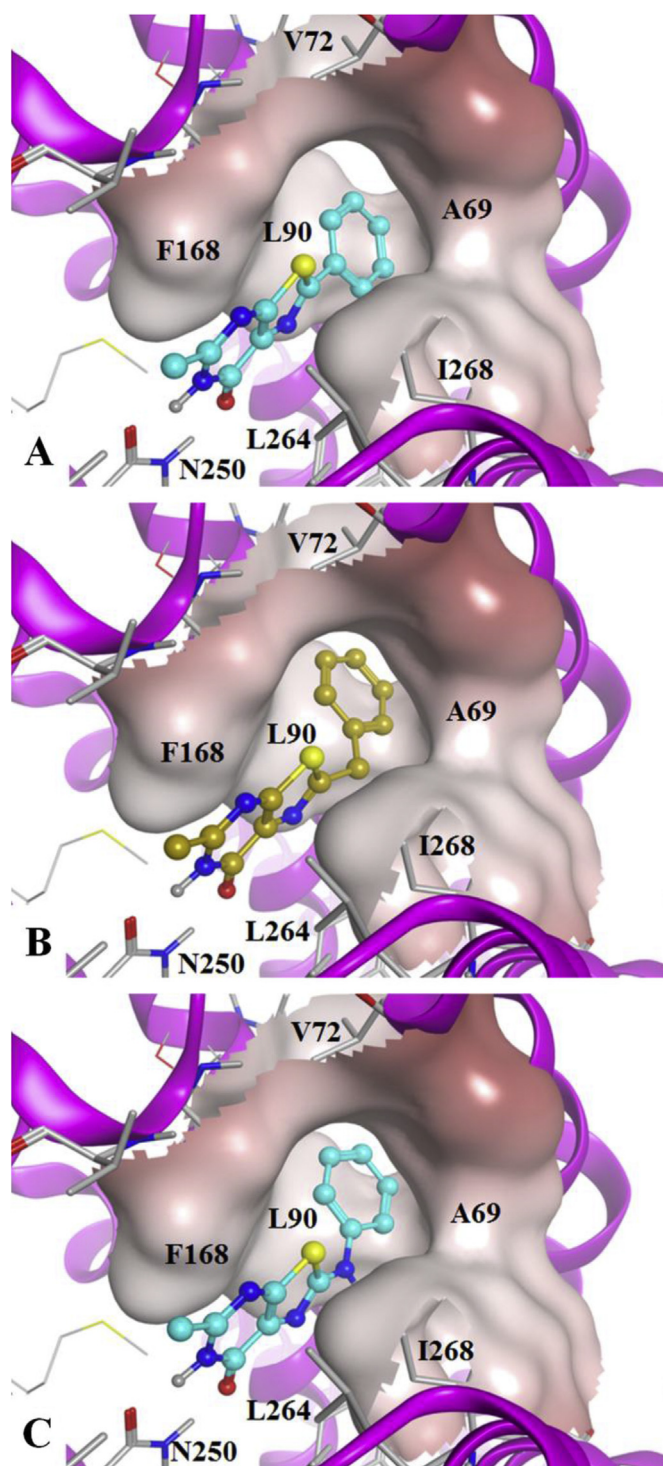


Fig. 4. A. Detail of the interaction of the 2-substituent with the TM2-TM3 residues (compounds **1**, **14**, and **21** are shown). The TM2-TM3 subcavity (see text for details) is represented as molecular surface.

score docking poses of each compound were subjected to energy minimization and then rescored using three available methods implemented in MOE: the *London dG* and the *Affinity dG* scoring tools and the *dock-pK_i* predictor (see experimental section for details). For each compound, the top-score docking poses, according to at least two out of three scoring functions, were selected for final ligand–target interaction analysis.

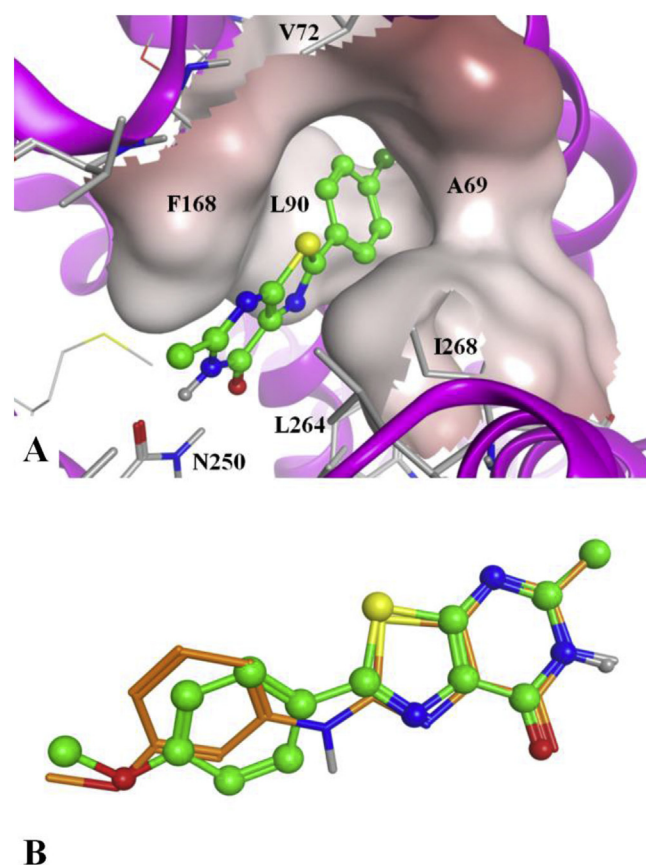


Fig. 5. A. Detail of the interaction of the 2-substituent with the TM2-TM3 residues (compound **4** is shown). The TM2-TM3 subcavity (see text for details) is represented as molecular surface. B. Superimposition of the compounds **2** and **25** binding mode. The methoxy group in position meta of the appended phenyl ring of compound **25** results superimposed to the same substituent in position para of the 2 phenyl ring of compound **2**.

The compounds are relatively small compared to the cavity volume, hence they may present different binding modes as evidenced by the docking results. The most populated (and lowest scoring) family of docking conformations presents the ligand almost orthogonally oriented with respect to the receptor axis (Fig. 3), with the bicyclic scaffold located in proximity of TM (transmembrane) domains 6 and 7 and EL (extracellular loop) 2 domain and the 2-substituent positioned between TM2 and TM3 segments. Thus, docking results suggest for the newly synthesized compounds a different binding mode than the above cited pyrazolopyrimidine derivatives (Series **PP**) from which these compounds were designed. In fact, the S-3 and N-4 atoms of the thiazolopyrimidine scaffold are oriented toward the extracellular environment, apparently not involved in any direct interaction with receptor residues, while the N-1 atom and the carbonyl group at 7-position point toward the core of the protein. The 7-oxo function and the NH group in 6-position make a double H-bond with the Asn250^{6,55} residue (as superscript it is indicated the residue ID according to the numbering system suggested by Ballesteros and Weinstein [48]). This interaction is the main polar interaction between the compounds and the receptor and hence seems the key stabilizing factor for this binding mode of the ligands.

The 2-substituent differently affects the affinity of the compounds on the basis of its volume and chemical-physical profile. When this substituent is an aromatic group directly bound to the scaffold (compounds **1–13** and **15–20**), the best affinity values are observed when this group presents a marked hydrophobic profile.

Hence, insertion in position 2 of a phenyl ring (compound **1**) or a para-substituted phenyl moiety presenting methoxy or methyl groups, or a chlorine atom (compounds **2**, **3**, **4**, respectively) leads to good affinity for the hA₃AR, while a fluorine atom or a trifluoromethyl, hydroxyl, or carboxy group at the same position leaves unchanged or decreases affinity at the same receptor. Docking results show that the 2-substituent is inserted into a narrow sub-pocket (Figs. 4 and 5A) given by residues belonging to TM2 (Val65^{2.57}, Leu68^{2.60}, Ala69^{2.61}, and Val72^{2.64}) and TM3 (Met86^{3.28} and Leu90^{3.32}). The chemical-physical profile of these residues provides a marked hydrophobic environment for this subpocket and explains why the insertion of too polar or hydrophilic groups is detrimental for the compound affinity. In this sense, the insertion of heterocycles presenting polar atoms (i.e. pyridyl or furyl groups as in compounds **15**–**17**) seems detrimental, while introduction of heterocycles with a more pronounced hydrophobic profile (i.e. thienyl or pyrrol-1-yl groups as in compounds **18**–**19**) maintains affinity for the receptor. Given the above cited interaction with the Asn250^{6.55} residue, which provide a first general stabilizing factor of this binding mode of the ligands, the geometric and chemical-physical matching of the 2-substituent and the TM2-TM3 subcavity provides the second stabilizing feature and also a factor providing high or low affinity of the analyzed compounds for the A₃AR. As indicated above, this subcavity is quite narrow and this feature explains why the presence of a fluorine atom at the meta-position of the 2-phenyl ring is accepted (compound **12**), while insertion, in the same position, of bigger functions like a methyl group or a chlorine atom (compounds **10**–**11**), leads to a drop of hA₃AR affinity, contrary to what is observed for the same kind of substitutions at the para-position.

When the aromatic group at position 2 is spaced from the thiazolopyrimidine scaffold by a methylene or amine linker as in compounds **14** and **21**–**28**, respectively, a general decrease in affinity is observed. Docking results suggest that introduction of the linker makes the phenyl ring being differently oriented than the analogue ring directly bound to the scaffold. Fig. 4 shows a comparison between the docking pose of compound **1** (whose phenyl ring is directly bound to the scaffold; Fig. 4A) and the binding mode of compounds **14** and **21** (whose phenyl ring is bound to the scaffold through a methyl or an amine as spacers; Fig. 4B and C, respectively). As a consequence, these compounds generally fail to match both the above cited stabilizing factors (the double H-bond with Asn250^{6.55} and the fitting into the TM2-TM3 subcavity). An exception is given when a small hydrophobic group is inserted at the meta-position of the appended phenyl ring (i.e. a methoxy or a methyl group as in compounds **25** and **26**, respectively). In this case, the small hydrophobic group gets similarly oriented to the analogue group inserted in para-position on the 2-phenyl ring directly bound to the bicyclic scaffold (Fig. 5, panel B). We must underline that this phenomenon is not observed for compound **27** which presents a chlorine atom at the meta-position of the 2-phenylamine substituent, but is not endowed with affinity for the receptor as the 2-(4-chlorophenyl) derivative **4**.

Finally, considering the derivatives presenting a 7-ethoxy function (compounds **29**–**33**), affinity for the A₃AR is observed only in the case of compound **33** presenting a methoxy group in the meta-position of the 2-phenylamine substituent. Respect to the 7-oxo analogue **25**, compound **33** lacks the H-bond donor function at position 6. The comparison of the affinity data of these two compounds suggests that the conversion of the 7-oxo function in a 7-ethoxy group and the consequent loss of an H-bond donor function in 6-position are not detrimental for the binding with the receptor. On the other hand, we cannot exclude that the two H-bond acceptor functions at position 6 and 7 of this ligand may interact with the amine function of Asn250^{6.55} sidechain. We

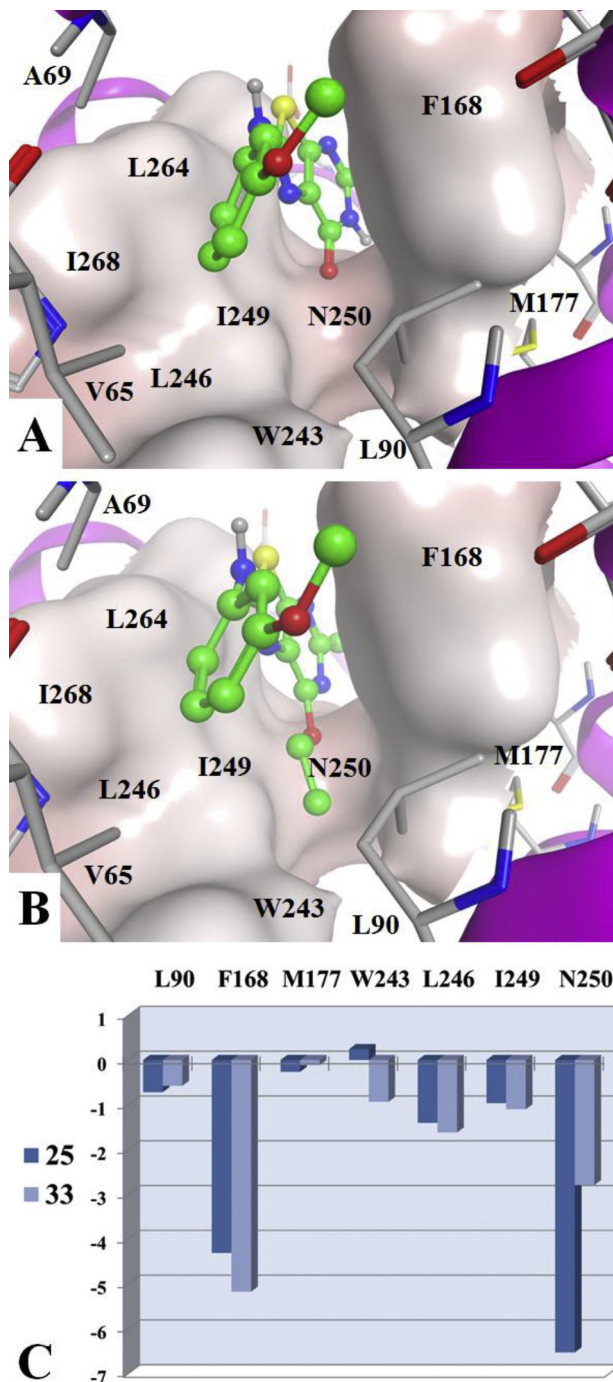


Fig. 6. Detail of the interaction of the 7-position of compounds **25** (A) and **33** (B) with the A₃AR residues. The A₃AR subcavity (see text for details) is represented as molecular surface. C. Interaction between the same two compounds and the A₃AR residues estimated by the *IF-E 6.0* tool; only residues in proximity of the compound 7-position are here considered.

compared the binding mode of these two compounds by considering the residues in proximity of the 6- and 7-position of the ligands. As described in Fig. 6(A–B), the introduction of an ethoxy group in 7-position (compound **33**, Fig. 6B) makes the ethyl chain being inserted within a set of hydrophobic aminoacids (Leu90^{3.32}, F168, M177^{5.38}, W243^{6.48}, L246^{6.51}, and Ile249^{6.54}). The interaction of compounds **25** and **33** with the surrounding residues was estimated with the aid of the *IF-E 6.0* tool [49] retrievable at the SVL exchange service (Chemical Computing Group, Inc. SVL

exchange: <http://svl.chemcomp.com>). The script calculates and displays atomic and residue interaction forces as 3D vectors. It also calculates the per-residue interaction energies (values in kcal mol⁻¹), where negative and positive energy values are associated to favorable and unfavorable interactions, respectively. This method was already used by us for the analysis of ligand–target interaction for a series of potent A₃AR and A_{2B}AR agonists [50,51]. Focusing in particular on the interaction between the 7-position and the surrounding A₃AR residues, results (Fig. 6C) show that as expected there is a quite stronger interaction between compound **25** and Asn250^{6,55} respect to compound **33**. At the same time it is also observable that for some residues the interaction is better with the latter compound (Phe168, W243^{6,48}, L246^{6,51}, and Ile249^{6,54}). This data could suggest on the one hand that the presence of a double H-bond interaction with Asn250^{6,55} (i.e. compound **25**) may be important in terms of stabilization of the binding mode and gain of high affinity, on the other hand that the conversion of the 7-oxo group in an ethoxy function (compound **33**) provides a more marked hydrophobic character that increase the interaction with non-polar residues of the cavity and possibly makes easier its desolvation during the process of interaction with the receptor. These considerations could be applied in general to all analogues presenting a different 7-group. Nevertheless, we must also note that docking results do not provide clear explanations regarding the loss of affinity of compounds **29–31**, while for compound **32** the same considerations as for compound **21** can be made.

4.3. Conclusion

In the present study we have identified the thiazolo[5,4-d]pyrimidin-7-one bicyclic system as a new scaffold for obtaining potent and selective hA₃ AR antagonists. In fact, some of the newly synthesized compounds showed high hA₃AR affinity and selectivity versus all the other AR subtypes, the best being the 2-(4-chlorophenyl)-5-methyl-thiazolo[5,4-d]pyrimidin-7-one **4** which possesses the highest hA₃AR affinity value ($K_i = 18$ nM). Molecular docking of the newly synthesized compounds allows us to represent their hypothetical binding mode to our hA₃ receptor model as well as to rationalize the observed SARs.

5. Experimental section

5.1. Chemistry

The microwave-assisted synthesis were performed using an Initiator EXP Microwave Biotage instrument (frequency of irradiation: 2.45 GHz). Analytical silica gel plates (Merck F254), preparative silica gel plates (Merck F254, 2 mm) and silica gel 60 (Merck, 70–230 mesh) were used for analytical and preparative TLC, and for column chromatography, respectively. All melting points were determined on a Gallenkamp melting point apparatus and are uncorrected. Elemental analyses were performed with a Flash E1112 Thermofinnigan elemental analyzer for C, H, N and the results were within ±0.4% of the theoretical values. The IR spectra were recorded with a Perkin–Elmer Spectrum RX I spectrometer in Nujol mulls and are expressed in cm⁻¹. The NMR spectra were obtained with a Bruker Avance 400 instrument (400 MHz for ¹H NMR and 100 MHz for ¹³C NMR). The chemical shifts are reported in δ (ppm) and are relative to the central peak of the solvent which was always DMSO-d₆. The following abbreviations are used: s = singlet, d = doublet, t = triplet, m = multiplet, br = broad, and ar = aromatic protons. Scanned ¹H and ¹³C NMR spectra of some selected compounds (**1**, **3**, **4**, **11**, **18**, **25**, **26**, **33**) are reported in the [Supplementary data](#).

5.1.1. General procedure for the synthesis of 2-(aroylamino)propanedioic acid diethyl ester derivatives (**34–35**, **46–47**)

The title compounds were prepared by reacting equimolar amounts of diethyl 2-aminomalonate hydrochloride (14.2 mmol) and the suitable aroyl chloride in anhydrous pyridine (30 mL). The mixture was stirred at room temperature for 2 h (compounds **34** and **35**) or 10 h (compounds **46** and **47**). Evaporation at reduced pressure of the solvent afforded a residue which was treated with H₂O (120 mL for compounds **34** and **35**, 40 mL for compounds **46** and **47**) and EtOH (5 mL). The resulting solid was collected by filtration, washed with water and recrystallised.

5.1.1.1. Diethyl ((phenylcarbonyl)amino)propanedioate **34 [31].** Yield 90%; m.p. 60–62 °C (Et₂O) (litt. m.p. 63 °C ethyl acetate/heptanes 1/10); ¹H NMR: 1.23 (t, 6H, 2 CH₃, J = 7.1 Hz), 4.15 (m, 4H, 2 CH₂), 5.31 (d, 1H, CH, J = 7.6 Hz), 7.50 (t, 2H, ar, J = 7.7 Hz), 7.59 (t, 1H, ar, J = 7.2 Hz), 7.91 (d, 2H, ar, J = 7.2 Hz), 9.31 (d, 1H, NH, J = 7.6 Hz). IR: 3312, 1747, 1639. Anal. Calc. for C₁₄H₁₇NO₅.

5.1.1.2. Diethyl (((4-methoxyphenyl)carbonyl)amino)propanedioate **35 [31].** Yield 89%; m.p. 103–107 °C (Et₂O) (litt. m.p. 106 °C); ¹H NMR: 1.23 (t, 6H, 2 CH₃, J = 7.1 Hz), 3.83 (s, 3H, OCH₃), 4.16–4.26 (m, 4H, 2 CH₂), 5.29 (d, 1H, CH, J = 7.5 Hz), 7.03 (d, 2H, ar, J = 8.9 Hz), 7.90 (d, 2H, ar, J = 8.9 Hz), 9.15 (d, 1H, NH, J = 7.5 Hz). IR: 3300, 1753, 1631. Anal. Calc. for C₁₅H₁₉NO₆.

5.1.1.3. Diethyl ((pyridin-3-ylcarbonyl)amino)propanedioate **46.** Yield 78%; m.p. 76–78 °C (Et₂O); ¹H NMR: 1.23 (t, 6H, 2 CH₃, J = 7.1 Hz), 4.17–4.26 (m, 4H, 2 CH₂), 5.34 (d, 1H, CH, J = 7.5 Hz), 7.57 (dd, 1H, ar, J = 7.7, 4.9 Hz), 8.27 (d, 1H, ar, J = 7.7 Hz), 8.77 (d, 1H, ar, J = 4.9 Hz), 9.05 (s, 1H, ar), 9.60 (d, 1H, NH, J = 7.5 Hz). IR: 3304, 1753, 1643. Anal. Calc. for C₁₃H₁₆N₂O₅.

5.1.1.4. Diethyl ((pyridin-4-ylcarbonyl)amino)propanedioate **47.** Yield 79%; m.p. 60–62 °C (Et₂O); ¹H NMR: 1.23 (t, 6H, 2 CH₃, J = 7.1 Hz), 4.12–4.26 (m, 4H, 2 CH₂), 5.33 (d, 1H, CH, J = 7.6 Hz), 7.81 (d, 2H, ar, J = 5.6 Hz), 8.77 (d, 2H, ar, J = 5.6 Hz), 9.68 (d, 1H, NH, J = 7.6 Hz). IR: 3313, 1743, 1645. Anal. Calc. for C₁₃H₁₆N₂O₅.

5.1.2. General procedure for the synthesis of 2-(aroylamino)propanedioic acid diethyl ester derivatives (**36–45**, **48–49**)

Suitable aroyl chloride (13.6 mmol) was added dropwise to a solution of diethyl aminomalonate hydrochloride (14.2 mmol) and sodium hydrogen carbonate (35.6 mmol) in Et₂O (40 mL) and H₂O (30 mL) cooled at 0 °C. The solution was warmed to room temperature and stirred for 2 h. The organic layer was washed with 1 M HCl (20 mL) then water (30 mL), dried (Na₂SO₄) and concentrated to give the desired amide which was collected by filtration and recrystallised.

5.1.2.1. Diethyl (((4-methylphenyl)carbonyl)amino)propanedioate **36 [32].** Yield 92%; m.p. 102–103 °C (Et₂O); ¹H NMR: 1.22 (t, 6H, 2 CH₃, J = 7.1 Hz), 3.37 (s, 3H, CH₃), 4.16–4.25 (m, 4H, 2 CH₂), 5.29 (d, 1H, CH, J = 7.5 Hz), 7.31 (d, 2H, ar, J = 8.0 Hz), 7.82 (d, 2H, ar, J = 8.0 Hz), 9.23 (d, 1H, NH, J = 7.5 Hz). IR: 3292, 1754, 1638. Anal. Calc. for C₁₅H₁₉NO₅.

5.1.2.2. Diethyl (((4-chlorophenyl)carbonyl)amino)propanedioate **37 [33].** Yield 93%; m.p. 91–94 °C (Et₂O); ¹H NMR: 1.23 (t, 6H, 2 CH₃, J = 7.1 Hz), 4.12–4.27 (m, 4H, 2 CH₂), 5.30 (d, 1H, CH, J = 7.5 Hz), 7.58 (d, 2H, ar, J = 8.5 Hz), 7.93 (d, 2H, ar, J = 8.5 Hz), 9.44 (d, 1H, NH, J = 7.5 Hz). IR: 3312, 1748, 1643. Anal. Calc. for C₁₄H₁₆ClNO₅.

5.1.2.3. Diethyl (((4-fluorophenyl)carbonyl)amino)propanedioate **38 [34].** Yield 90%; m.p. 79–81 °C (Et₂O) (litt. m.p. 108–109 °C); ¹H

NMR: 1.23 (t, 6H, 2 CH₃, *J* = 7.1 Hz), 4.14–4.27 (m, 4H, 2 CH₂), 5.30 (d, 1H, CH, *J* = 7.6 Hz), 7.34 (t, 2H, ar, *J* = 8.9 Hz), 7.99 (dd, 2H, ar, *J* = 5.4, 2.1 Hz), 9.39 (d, 1H, NH, *J* = 7.6 Hz). IR: 3358, 1751, 1658. Anal. Calc. for C₁₄H₁₆FNO₅.

5.1.2.4. Diethyl (((4-(trifluoromethyl)phenyl)carbonyl)amino)propanedioate **39.** Yield 92%; m.p. 103–105 °C (Et₂O); ¹H NMR: 1.23 (t, 6H, 2 CH₃, *J* = 7.1 Hz), 4.17–4.26 (m, 4H, 2 CH₂), 5.33 (d, 1H, CH, *J* = 7.5 Hz), 7.90 (d, 2H, ar, *J* = 8.0 Hz), 8.10 (d, 2H, ar, *J* = 8.0 Hz), 9.62 (d, 1H, NH, *J* = 7.5 Hz). IR: 3294, 1754, 1646. Anal. Calc. for C₁₅H₁₆F₃NO₅.

5.1.2.5. Diethyl (((3-methoxyphenyl)carbonyl)amino)propanedioate **40.** Yield 92%; m.p. 54–56 °C (Et₂O); ¹H NMR: 1.23 (t, 6H, 2 CH₃, *J* = 7.1 Hz), 3.82 (s, 3H, OCH₃), 4.15–4.27 (m, 4H, 2 CH₂), 5.31 (d, 1H, CH, *J* = 7.6 Hz), 7.15 (dd, 1H, ar, *J* = 5.7, 1.8 Hz), 7.39–7.51 (m, 3H, ar), 9.34 (d, 1H, NH, *J* = 7.6 Hz). IR: 3298, 1747, 1640 Anal. Calc. for C₁₅H₁₉FNO₆.

5.1.2.6. Diethyl (((3-methylphenyl)carbonyl)amino)propanedioate **41 [35].** Yield 91%; m.p. 53–56 °C (Et₂O); ¹H NMR: 1.23 (t, 6H, 2 CH₃, *J* = 7.1 Hz), 2.37 (s, 3H, CH₃), 4.16–4.27 (m, 4H, 2 CH₂), 5.31 (d, 1H, CH, *J* = 7.6 Hz), 7.36–7.39 (m, 2H, ar), 7.69–7.74 (m, 2H, ar), 9.24 (d, 1H, NH, *J* = 7.6 Hz). IR: 3281, 1753, 1642. Anal. Calc. for C₁₅H₁₉NO₅.

5.1.2.7. Diethyl (((3-chlorophenyl)carbonyl)amino)propanedioate **42.** Yield 94%; m.p. 84–86 °C (Et₂O); ¹H NMR: 1.23 (t, 6H, 2 CH₃, *J* = 7.1 Hz), 4.17–4.27 (m, 4H, 2 CH₂), 5.31 (d, 1H, CH, *J* = 7.5 Hz), 7.55 (t, 1H, ar, *J* = 7.9 Hz), 7.67 (dd, 1H, ar, *J* = 7.9, 1.7 Hz), 7.87 (d, 1H, ar, *J* = 7.9), 7.97 (d, 1H, ar, *J* = 1.7 Hz), 9.51 (d, 1H, NH, *J* = 7.5 Hz). IR: 3281, 1751, 1643. Anal. Calc. for C₁₄H₁₆ClNO₅.

5.1.2.8. Diethyl (((3-fluorophenyl)carbonyl)amino)propanedioate **43 [36].** Yield 89%; m.p. 72–74 °C (Et₂O); ¹H NMR: 1.23 (t, 6H, 2 CH₃, *J* = 7.1 Hz), 4.14–4.25 (m, 4H, 2 CH₂), 5.31 (d, 1H, CH, *J* = 7.6 Hz), 7.45 (t, 1H, ar, *J* = 8.6 Hz), 7.57 (dd, 1H, ar, *J* = 7.5, 6.2 Hz), 7.72 (d, 1H, ar, *J* = 10.0 Hz), 7.77 (d, 1H, ar, *J* = 7.0 Hz), 9.45 (d, 1H, NH, *J* = 7.6 Hz). IR: 3295, 1755, 1642. Anal. Calc. for C₁₄H₁₆FNO₅.

5.1.2.9. Diethyl (((3-(trifluoromethyl)phenyl)carbonyl)amino)propanedioate **44.** Yield 91%; m.p. 89–92 °C (Et₂O); ¹H NMR: 1.23 (t, 6H, 2 CH₃, *J* = 7.1 Hz), 4.16–4.28 (m, 4H, 2 CH₂), 5.35 (d, 1H, CH, *J* = 7.6 Hz), 7.77 (t, 1H, ar, *J* = 7.7 Hz), 7.98 (d, 1H, ar, *J* = 7.7 Hz), 8.21 (d, 1H, ar, *J* = 7.8 Hz), 8.27 (s, 1H, ar), 9.60 (d, 1H, NH, *J* = 7.6 Hz). IR: 3303, 1749, 1640. Anal. Calc. for C₁₅H₁₆F₃NO₅.

5.1.2.10. Diethyl ((phenylacetyl)amino)propanedioate **45 [37].** Yield 90%; m.p. 66–68 °C (Et₂O) (litt. m.p. 68 °C); ¹H NMR: 1.19 (t, 6H, 2 CH₃, *J* = 7.1 Hz), 3.58 (s, 2H, CH₂), 4.11–4.23 (m, 4H, 2 CH₂), 5.22 (d, 1H, CH, *J* = 7.5 Hz), 7.22–7.32 (m, 5H, ar), 9.02 (d, 1H, NH, *J* = 7.5 Hz) IR: 3316, 1746, 1648. Anal. Calc. for C₁₅H₁₉NO₅.

5.1.2.11. Diethyl ((furan-2-ylcarbonyl)amino)propanedioate **48.** Yield 88%; m.p. 60–63 °C (Et₂O); ¹H NMR: 1.22 (t, 6H, 2 CH₃, *J* = 7.1 Hz), 4.14–4.26 (m, 4H, 2 CH₂), 5.22 (d, 1H, CH, *J* = 7.5 Hz), 6.66–6.68 (m, 1H, ar), 7.29 (d, 1H, ar, *J* = 3.5 Hz), 7.91 (d, 1H, ar, *J* = 0.9 Hz), 9.05 (d, 1H, NH, *J* = 7.5 Hz). IR: 3335, 1749, 1651. Anal. Calc. for C₁₂H₁₅NO₆.

5.1.2.12. Diethyl ((thienyl-2-ylcarbonyl)amino)propanedioate **49.** Yield 91%; m.p. 74–77 °C (Et₂O); ¹H NMR: 1.23 (t, 6H, 2 CH₃, *J* = 7.1 Hz), 4.15–4.27 (m, 4H, 2 CH₂), 5.29 (d, 1H, CH, *J* = 7.8 Hz), 7.18–7.20 (m, 1H, ar), 7.83 (d, 1H, ar, *J* = 4.9 Hz), 7.97 (d, 1H, ar, *J* = 3.0 Hz), 9.36 (d, 1H, NH, *J* = 7.8 Hz). IR: 3281, 1734, 1632 Anal. Calc. for C₁₂H₁₅NO₅S.

5.1.3. General procedure for the synthesis of *N*-(4,6-dihydroxy-2-methylpyrimidin-5-yl)carboxamide derivatives (**50–65**)

A suspension of acetamide hydrochloride (15.6 mmol) and sodium (31.2 mmol) in ethanol (44 mL) was stirred at 30 °C for 10 min and then added with the suitable amide **34–49** (5.2 mmol). The reaction mixture was refluxed for 4 h then concentrated in vacuo. The solid product was filtered off, washed with ethanol, dissolved in the minimum amount of water (about 20 mL, 10 mL for compounds **62** and **63**) and acidified to pH 2–3 with 6 M HCl (to pH 4–5 with acetic acid for compounds **62** and **63**). The precipitate was collected, washed with acetone and recrystallised.

5.1.3.1. *N*-(4,6-dihydroxy-2-methylpyrimidin-5-yl)benzamide **50.** Yield 49%; m.p. >300 °C (acetic acid); ¹H NMR: 2.29 (s, 3H, CH₃), 7.48 (t, 2H, ar, *J* = 6.9 Hz), 7.55 (t, 1H, ar, *J* = 6.9 Hz), 7.94 (d, 2H, ar, *J* = 6.9 Hz), 9.07 (s, 1H, NH), 12.05 (br s, 2H, 2 OH). IR: 3258, 2670, 1641. Anal. Calc. for C₁₂H₁₁N₃O₃.

5.1.3.2. *N*-(4,6-dihydroxy-2-methylpyrimidin-5-yl)-4-methoxybenzamide **51.** Yield 52%; m.p. >300 °C (acetic acid); ¹H NMR: 2.29 (s, 3H, CH₃), 3.83 (s, 3H, OCH₃), 7.01 (d, 2H, ar, *J* = 8.4 Hz), 7.92 (d, 2H, ar, *J* = 8.4 Hz), 8.89 (s, 1H, NH), 12.01 (br s, 2H, 2 OH). IR: 3155, 2598, 1639; Anal. Calc. for C₁₃H₁₃N₃O₄.

5.1.3.3. *N*-(4,6-dihydroxy-2-methylpyrimidin-5-yl)-4-methylbenzamide **52.** Yield 53%; m.p. >300 °C (acetic acid); ¹H NMR: 2.28 (s, 3H, CH₃), 2.37 (s, 3H, CH₃), 7.28 (d, 2H, ar, *J* = 7.8 Hz), 7.85 (d, 2H, ar, *J* = 7.8 Hz), 8.98 (s, 1H, NH), 12.02 (br s, 2H, 2 OH). IR: 3230, 2617, 1644. Anal. Calc. for C₁₃H₁₃N₃O₃.

5.1.3.4. 4-Chloro-*N*-(4,6-dihydroxy-2-methylpyrimidin-5-yl)benzamide **53.** Yield 55%; m.p. >300 °C (acetic acid); ¹H NMR: 2.28 (s, 3H, CH₃), 7.56 (d, 2H, ar, *J* = 8.0 Hz), 7.96 (d, 2H, ar, *J* = 8.0 Hz), 9.16 (s, 1H, NH), 12.14 (br s, 2H, 2 OH). IR: 3236, 2603, 1643. Anal. Calc. for C₁₂H₁₀ClN₃O₃.

5.1.3.5. *N*-(4,6-dihydroxy-2-methylpyrimidin-5-yl)-4-fluorobenzamide **54 [40].** Yield 53%; m.p. >300 °C (acetic acid); ¹H NMR: 2.28 (s, 3H, CH₃), 7.31 (t, 2H, ar, *J* = 8.7 Hz), 8.01 (t, 2H, ar, *J* = 5.9 Hz), 9.12 (s, 1H, NH), 12.06 (br s, 2H, 2 OH). IR: 3240, 2610, 1645. Anal. Calc. for C₁₂H₁₀FN₃O₃.

5.1.3.6. *N*-(4,6-dihydroxy-2-methylpyrimidin-5-yl)-4-(trifluoromethyl)benzamide **55.** Yield 54%; m.p. >300 °C (acetic acid); ¹H NMR: 2.29 (s, 3H, CH₃), 7.87 (d, 2H, ar, *J* = 8.0 Hz), 8.13 (d, 2H, ar, *J* = 8.0 Hz), 9.33 (s, 1H, NH), 12.32 (br s, 2H, 2 OH). Anal. 3243, 2618, 1634. Calc. for C₁₃H₁₀F₃N₃O₃.

5.1.3.7. *N*-(4,6-dihydroxy-2-methylpyrimidin-5-yl)-3-methoxybenzamide **56.** Yield 46%; m.p. 288–290 °C (acetic acid); ¹H NMR: 2.28 (s, 3H, CH₃), 3.82 (s, 3H, OCH₃), 7.10 (d, 1H, ar, *J* = 8.2 Hz), 7.38 (t, 1H, ar, *J* = 7.8 Hz), 7.49–7.53 (m, 2H, ar), 9.05 (s, 1H, NH), 12.01 (br s, 2H, 2 OH). IR: 3152, 2630, 1639. Anal. Calc. for C₁₃H₁₃N₃O₄.

5.1.3.8. *N*-(4,6-dihydroxy-2-methylpyrimidin-5-yl)-3-methylbenzamide **57.** Yield 55%; m.p. >300 °C (acetic acid); ¹H NMR: 2.28 (s, 3H, CH₃), 2.37 (s, 3H, CH₃), 7.35–7.36 (m, 2H, ar), 7.73–7.77 (m, 2H, ar), 9.00 (s, 1H, NH), 12.01 (br s, 2H, 2 OH). IR: 3251, 2611, 1624. Anal. Calc. for C₁₃H₁₃N₃O₃.

5.1.3.9. 3-Chloro-*N*-(4,6-dihydroxy-2-methylpyrimidin-5-yl)benzamide **58.** Yield 54%; m.p. >300 °C (acetic acid); ¹H NMR: 2.28 (s, 3H, CH₃), 7.52 (t, 1H, ar, *J* = 7.9 Hz), 7.62 (d, 1H, ar, *J* = 8.0 Hz), 7.90 (d, 2H, ar, *J* = 7.8 Hz), 7.98 (s, 1H, ar), 9.20 (s, 1H, NH), 12.07 (br s, 2H, 2 OH).

IR: 3255, 2621, 1644. Anal. Calc. for $C_{12}H_{10}ClN_3O_3$.

5.1.3.10. *N*-(4,6-dihydroxy-2-methylpyrimidin-5-yl)-3-fluorobenzamide **59**. Yield 52%; m.p. >300 °C (acetic acid); 1H NMR: 2.29 (s, 3H, CH₃), 7.40 (t, 1H, ar, $J = 7.9$ Hz), 7.54 (dd, 1H, ar, $J = 14.0$, 7.5 Hz), 7.73 (d, 2H, ar, $J = 9.3$ Hz), 7.80 (d, 1H, ar, $J = 7.5$ Hz), 9.15 (s, 1H, NH), 12.08 (br s, 2H, 2 OH). IR: 3242, 2614, 1643. Anal. Calc. for $C_{12}H_{10}FN_3O_3$.

5.1.3.11. *N*-(4,6-dihydroxy-2-methylpyrimidin-5-yl)-3-(trifluoromethyl)benzamide **60**. Yield 51%; m.p. >300 °C (acetic acid); 1H NMR: 2.28 (s, 3H, CH₃), 7.74 (t, 1H, ar, $J = 7.7$ Hz), 7.93 (t, 1H, ar, $J = 7.5$ Hz), 8.24 (d, 2H, ar, $J = 8.00$ Hz), 8.29 (s, 1H, ar), 9.37 (s, 1H, NH), 12.16 (br s, 2H, 2 OH). IR: 3371, 2680, 1625. Anal. Calc. for $C_{13}H_{10}F_3N_3O_3$.

5.1.3.12. *N*-(4,6-dihydroxy-2-methylpyrimidin-5-yl)-2-phenylacetamide **61**. Yield 48%; m.p. >300 °C (acetic acid); 1H NMR: 2.24 (s, 3H, CH₃), 3.58 (s, 2H, CH₂), 7.22–7.32 (m, 5H, ar), 8.91 (s, 1H, NH), 11.96 (br s, 2H, 2 OH). IR: 3256, 2610, 1630. Anal. Calc. for $C_{13}H_{13}N_3O_3$.

5.1.3.13. *N*-(4,6-dihydroxy-2-methylpyrimidin-5-yl)pyridine-3-carboxamide **62**. Yield 47%; m.p. >300 °C (acetic acid); 1H NMR: 2.29 (s, 3H, CH₃), 7.53 (s, 1H, ar), 8.27 (d, 1H, ar, $J = 7.4$ Hz), 8.73 (s, 2H, ar), 9.09 (s, 1H, ar), 9.29 (s, 1H, NH), 12.08 (br s, 2H, 2 OH). IR: 3349, 2678, 1640. Anal. Calc. for $C_{11}H_{10}N_4O_3$.

5.1.3.14. *N*-(4,6-dihydroxy-2-methylpyrimidin-5-yl)pyridine-4-carboxamide **63**. Yield 49%; m.p. >300 °C (acetic acid); 1H NMR: 2.25 (s, 3H, CH₃), 7.84 (d, 2H, ar, $J = 5.1$ Hz), 8.73 (d, 2H, ar, $J = 5.1$ Hz), 9.31 (s, 1H, NH), 11.98 (br s, 2H, 2 OH). IR: 3422, 3242, 2722, 1658. Anal. Calc. for $C_{11}H_{10}N_4O_3$.

5.1.3.15. *N*-(4,6-dihydroxy-2-methylpyrimidin-5-yl)furan-2-carboxamide **64**. Yield 48%; m.p. >300 °C (acetic acid); 1H NMR: 2.27 (s, 3H, CH₃), 6.64 (s, 1H, ar), 7.21 (d, 1H, ar, $J = 2.2$ Hz), 7.85 (s, 1H, ar), 8.88 (s, 1H, NH), 12.06 (br s, 2H, 2 OH). IR: 3259, 2640, 1642. Anal. Calc. for $C_{10}H_9N_3O_4$.

5.1.3.16. *N*-(4,6-dihydroxy-2-methylpyrimidin-5-yl)thiophene-2-carboxamide **65**. Yield 49%; m.p. >300 °C (acetic acid); 1H NMR: 2.28 (s, 3H, CH₃), 7.17 (t, 1H, ar, $J = 7.0$ Hz), 7.77 (d, 1H, ar, $J = 4.9$ Hz), 7.91 (d, 1H, ar, $J = 2.9$ Hz), 9.09 (s, 1H, NH), 12.17 (br s, 2H, 2 OH). IR: 3218, 2679, 1628. Anal. Calc. for $C_{10}H_9N_3O_3S$.

5.1.4. General procedure for the synthesis of 2-(alkyl)aryl-5-methyl-thiazolo[5,4-d]pyrimidin-7-one derivatives (**1–6**, **9–18**)

A suspension of the suitable *N*-(4,6-dihydroxy-2-methylpyrimidin-5-yl)carboxamide **50–65** (3.7 mmol) and phosphorus pentasulfide (8.5 mmol) in anhydrous pyridine (20 mL) was refluxed for 4–6 h. The solvent was evaporated in vacuo and the residue was treated with water (100 mL, 25 mL for compounds **15** and **16**). The resulting solid was filtered off and then refluxed for 6 h with conc HCl (0.3 mL) in NMP (8 mL). The mixture was cooled to room temperature and added with brine (100 mL) to afford a solid which was collected by filtration. The product was dissolved in 1.5 M NaOH (30 mL) and to this solution, maintained at room temperature, a water solution of H₂O₂ (35% H₂O₂ 0.93 mL, H₂O 5 mL) was added dropwise. The mixture was stirred at room temperature for 1–2 h and then acidified to pH 2–3 with 6 M HCl (to pH 4–5 with acetic acid, for compounds **15** and **16**). The resulting solid was collected by filtration, washed with water, and recrystallised.

5.1.4.1. 5-Methyl-2-phenyl-thiazolo[5,4-d]pyrimidin-7-one **1**. Yield 72%; m.p. >300 °C (acetic acid); 1H NMR: 2.42 (s, 3H, CH₃), 7.56–7.57 (m, 3H, ar), 7.99–8.01 (m, 2H, ar), 12.77 (br s, 1H, NH). ^{13}C NMR: 162.53, 162.29, 157.28, 156.80, 137.28, 133.04, 131.62, 129.84 (2C), 127.07 (2C), 21.58. IR: 1662, 1592. Anal. Calc. for $C_{12}H_9N_3OS$.

5.1.4.2. 2-(4-Methoxyphenyl)-5-methyl-thiazolo[5,4-d]pyrimidin-7-one **2**. Yield 80%; m.p. >300 °C (acetic acid); 1H NMR: 2.40 (s, 3H, CH₃), 3.85 (s, 3H, OCH₃), 7.11 (d, 2H, ar, $J = 8.8$ Hz), 7.94 (d, 2H, ar, $J = 8.8$ Hz), 12.72 (br s, 1H, NH). IR: 1692, 1604. Anal. Calc. for $C_{13}H_{11}N_3O_2S$.

5.1.4.3. 5-Methyl-2-(4-methylphenyl)-thiazolo[5,4-d]pyrimidin-7-one **3**. Yield 69%; m.p. >300 °C (acetic acid); 1H NMR: 2.39 (s, 3H, CH₃), 2.41 (s, 3H, CH₃), 7.37 (d, 2H, ar, $J = 8.0$ Hz), 7.89 (d, 2H, ar, $J = 8.0$ Hz), 12.75 (br s, 1H, NH). ^{13}C NMR: 162.68, 162.08, 157.14, 156.78, 141.72, 137.22, 130.48, 130.40 (2C), 127.04 (2C), 21.58, 21.47. IR: 1689, 1601. Anal. Calc. for $C_{13}H_{11}N_3OS$.

5.1.4.4. 2-(4-Chlorophenyl)-5-methyl-thiazolo[5,4-d]pyrimidin-7-one **4**. Yield 82%; m.p. >300 °C (acetic acid); 1H NMR: 2.42 (s, 3H, CH₃), 7.63 (d, 2H, ar, $J = 8.6$ Hz), 8.02 (d, 2H, ar, $J = 8.6$ Hz), 12.78 (br s, 1H, NH). ^{13}C NMR: 162.53, 161.18, 157.53, 156.76, 137.32, 136.22, 131.89, 129.92 (2C), 128.77 (2C), 21.61. IR: 1690, 1595. Anal. Calc. for $C_{12}H_8ClN_3OS$.

5.1.4.5. 2-(4-Fluorophenyl)-5-methyl-thiazolo[5,4-d]pyrimidin-7-one **5**. Yield 76%; m.p. >300 °C (acetic acid); 1H NMR: 2.41 (s, 3H, CH₃), 7.39–7.43 (m, 2H, ar), 8.05–8.07 (m, 2H, ar), 12.75 (br s, 1H, NH). IR: 1693, 1591. Anal. Calc. for $C_{12}H_8FN_3OS$.

5.1.4.6. 5-Methyl-2-(4-trifluoromethyl-phenyl)-thiazolo[5,4-d]pyrimidin-7-one **6**. Yield 74%; m.p. >300 °C (acetic acid); 1H NMR: 2.43 (s, 3H, CH₃), 7.92 (d, 2H, ar, $J = 7.9$ Hz), 8.21 (d, 2H, ar, $J = 7.9$ Hz), 12.83 (br s, 1H, NH). IR: 1682, 1594. Anal. Calc. for $C_{13}H_8F_3N_3OS$.

5.1.4.7. 2-(3-Methoxyphenyl)-5-methyl-thiazolo[5,4-d]pyrimidin-7-one **9**. Yield 71%; m.p. >300 °C (acetic acid); 1H NMR: 2.41 (s, 3H, CH₃), 3.87 (s, 3H, OCH₃), 7.14 (dd, 1H, ar, $J = 5.7$, 2.5 Hz), 7.45–7.56 (m, 3H, ar), 12.75 (br s, 1H, NH). IR: 1688, 1596. Anal. Calc. for $C_{13}H_{11}N_3O_2S$.

5.1.4.8. 5-Methyl-2-(3-methylphenyl)-thiazolo[5,4-d]pyrimidin-7-one **10**. Yield 74%; m.p. >300 °C (acetic acid); 1H NMR: 2.41 (s, 6H, CH₃), 7.37–7.39 (m, 1H, ar), 7.50 (t, 1H, ar, $J = 7.6$ Hz), 7.68–7.83 (m, 2H, ar), 12.76 (br s, 1H, NH). IR: 1669, 1595. Anal. Calc. for $C_{13}H_{11}N_3OS$.

5.1.4.9. 2-(3-Chlorophenyl)-5-methyl-thiazolo[5,4-d]pyrimidin-7-one **11**. Yield 76%; m.p. >300 °C (acetic acid); 1H NMR: 2.42 (s, 3H, CH₃), 7.57–7.64 (m, 2H, ar), 7.96 (d, 1H, ar, $J = 7.3$ Hz), 8.02 (s, 1H, ar), 12.80 (br s, 1H, NH). ^{13}C NMR: 160.70, 157.65, 156.76, 134.90, 134.56, 131.76, 131.26, 126.30 (2C), 125.84 (2C), 21.62. IR: 1681, 1590. Anal. Calc. for $C_{12}H_8ClN_3OS$.

5.1.4.10. 2-(3-Fluorophenyl)-5-methyl-thiazolo[5,4-d]pyrimidin-7-one **12**. Yield 78%; m.p. >300 °C (acetic acid); 1H NMR: 2.42 (s, 3H, CH₃), 7.40–7.44 (m, 1H, ar), 7.59–7.64 (m, 1H, ar), 7.80–7.86 (m, 2H, ar), 12.81 (br s, 1H, NH). IR: 1670, 1587. Anal. Calc. for $C_{12}H_8FN_3OS$.

5.1.4.11. 5-Methyl-2-(3-trifluoromethyl-phenyl)-thiazolo[5,4-d]pyrimidin-7-one **13**. Yield 75%; m.p. >300 °C (acetic acid); 1H NMR: 2.43 (s, 3H, CH₃), 7.81–7.83 (m, 1H, ar), 7.93–7.95 (m, 1H, ar), 8.28 (s, 2H, ar), 12.84 (br s, 1H, NH). IR: 1694, 1592. Anal. Calc. for $C_{13}H_8F_3N_3OS$.

5.1.4.12. 2-Benzyl-5-methyl-thiazolo[5,4-d]pyrimidin-7-one 14. Yield 80%; m.p. 239–241 °C (methanol); ¹H NMR: 2.36 (s, 3H, CH₃), 4.38 (s, 2H, CH₂), 7.27–7.32 (m, 1H, ar), 7.36–7.37 (m, 4H, ar), 12.64 (br s, 1H, NH). IR: 1676, 1587. Anal. Calc. for C₁₃H₁₁N₃OS.

5.1.4.13. 5-Methyl-2-(pyridin-3-yl)-thiazolo[5,4-d]pyrimidin-7-one 15. Yield 58%; m.p. >300 °C (2-methoxyethanol); ¹H NMR: 2.43 (s, 3H, CH₃), 7.59–7.62 (m, 1H, ar), 8.37 (d, 1H, ar, *J* = 8.0 Hz), 8.73 (d, 1H, ar, *J* = 4.6 Hz), 9.17 (s, 1H, ar), 12.83 (br s, 1H, NH). IR: 1701, 1586. Anal. Calc. for C₁₁H₈N₄OS.

5.1.4.14. 5-Methyl-2-(pyridin-4-yl)-thiazolo[5,4-d]pyrimidin-7-one 16. Yield 55%; m.p. >300 °C (2-methoxyethanol); ¹H NMR: 2.43 (s, 3H, CH₃), 7.95 (d, 2H, ar), 8.77 (d, 2H, ar), 12.87 (br s, 1H, NH). IR: 1705, 1592. Anal. Calc. for C₁₁H₈N₄OS.

5.1.4.15. 2-(Furan-2-yl)-5-methyl-thiazolo[5,4-d]pyrimidin-7-one 17. Yield 71%; m.p. >300 °C (acetic acid); ¹H NMR: 2.40 (s, 3H, CH₃), 6.78 (s, 1H, ar), 7.28–7.29 (m, 1H, ar), 7.98 (s, 1H, ar), 12.76 (br s, 1H, NH). IR: 1662, 1592. Anal. Calc. for C₁₀H₇N₃O₂S.

5.1.4.16. 5-Methyl-2-(thiophen-2-yl)-thiazolo[5,4-d]pyrimidin-7-one 18. Yield 73%; m.p. >300 °C (acetic acid); ¹H NMR: 2.40 (s, 3H, CH₃), 7.22 (t, 1H, ar, *J* = 3.8 Hz), 7.77 (d, 1H, ar, *J* = 3.8 Hz), 7.85 (d, 1H, ar, *J* = 4.2 Hz), 12.77 (br s, 1H, NH). ¹³C NMR: 162.02, 157.30, 156.53, 156.42, 136.68, 136.62, 130.96, 129.50, 129.08, 21.56. IR: 1672, 1592. Anal. Calc. for C₁₀H₇N₃O₂S.

5.1.5. 2-(4-Hydroxyphenyl)-5-methyl-thiazolo[5,4-d]pyrimidin-7-one 7

A 1 M solution of BBr₃ in dichloromethane (2.9 mL) was added to a suspension of compound **2** (0.48 mmol) in anhydrous dichloromethane (70 mL). The resulting mixture was refluxed, under nitrogen atmosphere, for 24 h. The suspension was added with brine (100 mL) and stirred at room temperature for 30 min. The organic solvent was removed under reduced pressure and the precipitate was collected, washed with diethyl ether and recrystallised. Yield 48%; m.p. >300 °C (acetic acid); ¹H NMR: 2.39 (s, 3H, CH₃), 6.91 (d, 2H, ar, *J* = 8.8 Hz), 7.82 (d, 2H, ar, *J* = 8.8 Hz), 10.21 (br s, 1H, OH), 12.70 (br s, 1H, NH). IR: 1669, 1599. Anal. Calc. for C₁₂H₉N₃O₂S.

5.1.6. 4-(5-Methyl-7-oxo-6,7-dihydro-thiazolo[5,4-d]pyrimidin-2-yl)-benzoic acid 8

To a suspension of compound **3** (1.6 mmol) in conc H₂SO₄ (3.8 mL), maintained at room temperature, a solution of CrO₃ (14.8 mmol) in H₂O (4.2 mL) was slowly added. The reaction mixture was stirred at room temperature for 2 h, and then was added with H₂O (100 mL). The precipitate was collected by filtration, washed with H₂O and recrystallised. Yield 65%; m.p. >300 °C (acetic acid); ¹H NMR: 2.43 (s, 3H, CH₃), 8.04–8.20 (m, 4H, ar), 12.82 (br s, 1H, NH), 13.25 (br s, 1H, OH). IR: 1685, 1596. Anal. Calc. for C₁₃H₉N₃O₃S.

5.1.7. N-(7-Chloro-5-methyl-thiazolo[5,4-d]pyrimidin-2-yl) benzamide 66

The title compound was obtained by refluxing for 3 h a suspension of equimolar amounts of 5-amino-4,6-dichloro-2-methylpyrimidine (5.6 mmol) and benzoylthiocyanate in acetone (10 mL). The mixture was cooled to room temperature and the solid was filtered off and recrystallised. Yield 87%; m.p. 258–260 °C (ethanol); ¹H NMR: 2.72 (s, 3H, CH₃), 7.60 (t, 2H, ar, *J* = 7.4 Hz), 7.71 (t, 1H, ar, *J* = 7.4 Hz), 8.18 (d, 2H, ar, *J* = 7.4 Hz), 13.50 (s, 1H, NH). IR: 3182, 1666. Anal. Calc. for C₁₃H₉ClN₄OS.

5.1.8. 2-Amino-5-Methyl-thiazolo[5,4-d]pyrimidin-7-one 67

A suspension of compound **66** (1.6 mmol) in 6 M HCl (20 mL) was refluxed for 48 h. The solution was concentrated to half of its original volume, and then neutralized with NaHCO₃ saturated solution to give a solid which was collected, washed with water, and recrystallised. Yield 65%; m.p. >300 °C (ethanol); ¹H NMR: 2.28 (s, 3H, CH₃), 7.38 (s, 2H, NH₂), 12.27 (s, 1H, NH). IR: 3346, 3253, 3136, 1651. Anal. Calc. for C₆H₆N₄OS.

5.1.9. 5-Methyl-2-(1H-pyrrol-1-yl)-thiazolo[5,4-d]pyrimidin-7-one 19

To a hot (90 °C) solution of compound **67** (0.8 mmol) in acetic acid (10 mL), a solution of 2,5-diethoxytetrahydrofuran (2.5 mmol) in acetic acid (5 mL) was added dropwise. The reaction mixture was heated at 90 °C for 40 min and then cooled. The precipitate was collected, washed with diethyl ether, and recrystallised. Yield 53%; m.p. >300 °C (acetic acid); ¹H NMR: 2.17 (s, 3H, CH₃), 6.41 (t, 2H, ar, *J* = 1.8 Hz), 7.54 (t, 2H, ar, *J* = 1.9 Hz), 12.76 (br s, 1H, NH). IR: 1665. Anal. Calc. for C₁₀H₈N₄OS.

5.1.10. 2-(1H-Imidazol-1-yl)-5-methyl-thiazolo[5,4-d]pyrimidin-7-one 20

Aqueous formaldehyde (37%, 1.2 mmol), aqueous glyoxal (40%, 1.2 mmol), and ammonium acetate (1.2 mmol) were added to a suspension of compound **67** (1.2 mmol) in acetic acid (7 mL). The mixture was heated at 70 °C for 2 h and then cooled to room temperature and neutralized with NaHCO₃ saturated solution. The solid was collected, washed with water, and recrystallised. Yield 72%; m.p. >300 °C (2-methoxyethanol); ¹H NMR: 2.41 (s, 3H, CH₃), 7.21 (s, 1H, ar), 7.92 (s, 1H, ar), 8.50 (s, 1H, ar), 12.85 (s, 1H, NH). IR: 1689, 1581. Anal. Calc. for C₉H₇N₅OS.

5.1.11. General procedure for the synthesis of N-aryl-7-chloro-5-methyl-thiazolo[5,4-d]pyrimidin-2-amines 68–75

To a solution of 5-amino-4,6-dichloro-2-methyl-pyrimidine (5.6 mmol) in acetonitrile (20 mL), Cs₂CO₃ (11.2 mmol) and the suitable arylisothiocyanate (5.6 mmol) were added. The suspension was stirred at 50 °C until disappearance (5–30 h) of the starting materials (TLC monitoring: eluting system cyclohexane/ethyl acetate 7:3). Then, another 50 mL of acetonitrile was added and the suspension was heated at 50 °C and filtered while hot. The filtrate, after the addition of 5 g of silica gel (70–230 mesh), was stirred at room temperature for 20 min and filtered. The solvent was removed in vacuum, and the residue was collected and recrystallized.

5.1.11.1. 7-Chloro-5-methyl-N-phenyl-thiazolo[5,4-d]pyrimidin-2-amine 68. Reaction time 20 h. Yield 65%; m.p. 217–218 °C (ethanol); ¹H NMR: 2.63 (s, 3H, CH₃), 7.13 (t, 1H, ar, *J* = 7.4 Hz), 7.43 (t, 2H, ar, *J* = 8.2 Hz), 7.77 (d, 2H, ar, *J* = 8.2 Hz), 11.08 (s, 1H, NH). IR: 3255, 3197, 1584, 1446. Anal. calc. for C₁₂H₉ClN₄S

5.1.11.2. 7-Chloro-N-(4-methoxyphenyl)-5-methyl-thiazolo[5,4-d]pyrimidin-2-amine 69. Reaction time 30 h. Yield 75%; m.p. 208–209 dec °C (ethanol); ¹H NMR: 2.61 (s, 3H, CH₃), 3.77 (s, 3H, OCH₃), 7.01 (d, 2H, ar, *J* = 8.0 Hz), 7.66 (d, 2H, ar, *J* = 8.0 Hz), 10.91 (s, 1H, NH). IR: 3256, 1511, 1463. Anal. calc. for C₁₃H₁₁ClN₄OS.

5.1.11.3. 7-Chloro-5-methyl-N-(4-methylphenyl)-thiazolo[5,4-d]pyrimidin-2-amine 70. Reaction time 30 h. Yield 48%; m.p. 212–213 °C (ethanol); ¹H NMR: 2.30 (s, 3H, CH₃), 2.62 (s, 3H, CH₃), 7.22 (d, 2H, ar, *J* = 8.3 Hz), 7.63 (d, 2H, ar, *J* = 8.3 Hz), 10.98 (s, 1H, NH). IR: 3235, 1621, 1458. Anal. calc. for C₁₃H₁₁ClN₄S.

5.1.11.4. 7-Chloro *N*-(4-chlorophenyl)-5-methyl-thiazolo[5,4-*d*]pyrimidin-2-amine **71**. Reaction time 6 h. Yield 51%; m.p. 216–217 °C (ethanol); ¹H NMR: 2.63 (s, 3H, CH₃), 7.48 (d, 2H, ar, *J* = 8.8 Hz), 7.80 (d, 2H, ar, *J* = 8.8 Hz), 11.20 (s, 1H, NH). IR: 3264, 1625, 1462. Anal. calc. for C₁₂H₈Cl₂N₄S.

5.1.11.5. 7-Chloro-*N*-(3-methoxyphenyl)-5-methyl-thiazolo[5,4-*d*]pyrimidin-2-amine **72**. Reaction time 20 h. Yield 73%; m.p. 206–207 °C (ethanol); ¹H NMR: 2.63 (s, 3H, CH₃), 3.79 (s, 3H, OCH₃), 6.70 (dd, 1H, ar, *J* = 8.1, 1.9 Hz), 7.20 (dd, 1H, ar, *J* = 8.1, 1.9 Hz), 7.32 (t, 1H, ar, *J* = 8.1 Hz), 7.59 (t, 1H, ar, *J* = 2.0 Hz), 11.08 (s, 1H, NH). IR: 3198, 1577, 1438. Anal. calc. for C₁₃H₁₁ClN₄O₂S.

5.1.11.6. 7-Chloro-5-methyl-*N*-(3-methylphenyl)-thiazolo[5,4-*d*]pyrimidin-2-amine **73**. Reaction time 21 h. Yield 76%; m.p. 240–241 dec °C (ethanol); ¹H NMR: 2.34 (s, 3H, CH₃), 2.62 (s, 3H, CH₃), 6.95 (d, 1H, ar, *J* = 7.2 Hz), 7.31 (t, 1H, ar, *J* = 7.6 Hz), 7.52 (s, 1H, ar), 7.63 (d, 1H, ar, *J* = 7.6 Hz), 11.01 (s, 1H, NH). IR: 3246, 1560, 1462. Anal. calc. for C₁₃H₁₁ClN₄S.

5.1.11.7. 7-Chloro-*N*-(3-chlorophenyl)-5-methyl-thiazolo[5,4-*d*]pyrimidin-2-amine **74**. Reaction time 24 h. Yield 47%; m.p. 244–245 dec °C (ethanol); ¹H NMR: 2.64 (s, 3H, CH₃), 7.17 (dd, 1H, ar, *J* = 8.0, 1.0 Hz), 7.44 (t, 1H, ar, *J* = 8.0 Hz), 7.60 (dd, 1H, ar, *J* = 8.0, 1.0 Hz), 8.04 (s, 1H, ar), 11.26 (s, 1H, NH). IR: 3246, 1429, 1577. Anal. calc. for C₁₂H₈Cl₂N₄S.

5.1.11.8. 7-Chloro-*N*-(3,4-dichlorophenyl)-5-methyl-thiazolo[5,4-*d*]pyrimidin-2-amine **75**. Reaction time 5 h. Yield 52%; m.p. 243–244 °C (ethanol); ¹H NMR (DMSO-*d*₆): 2.64 (s, 3H, CH₃), 7.61–7.68 (m, 2H, ar), 8.25 (d, 1H, ar, *J* = 2.4 Hz), 11.36 (s, 1H, NH). IR: 3266, 1624, 1578, 1460. Anal. calc. for C₁₂H₇Cl₃N₄S.

5.1.12. General procedure for the synthesis of 2-arylamino-5-methyl-thiazolo[5,4-*d*]pyrimidin-7-ones **21–28**

Sodium acetate (2.9 mmol) was added to a suspension of the suitable *N*-aryl-7-chloro-5-methyl-[1,3]thiazolo[5,4-*d*]pyrimidin-2-amine **68–75** (1.4 mmol) in acetic acid (10 mL). The suspension was refluxed 18–28 h (compounds **21–22**, **25–26**) or microwave irradiated at 140 °C for 30–60 min (compounds **23–24**, **27–28**). The mixture was cooled at room temperature, the crude product was collected by filtration, washed with water and recrystallized.

5.1.12.1. 5-Methyl-2-(phenylamino)-thiazolo[5,4-*d*]pyrimidin-7-one **21**. Reaction time 18 h. Yield 82%; m.p. >300 °C (2-methoxyethanol); ¹H NMR: 2.34 (s, 3H, CH₃), 7.02 (t, 1H, ar, *J* = 7.7 Hz), 7.35 (t, 2H, ar, *J* = 8.0 Hz), 7.71 (d, 2H, ar, *J* = 8.0), 10.45 (s, 1H, NH), 12.50 (broad s, 1H, NH). IR: 3489, 3245, 1669. Anal. calc. for C₁₂H₁₀N₄O₂S.

5.1.12.2. 2-((4-Methoxyphenyl)amino)-5-methyl-thiazolo[5,4-*d*]pyrimidin-7-one **22**. Reaction time 19 h. Yield 61%; m.p. >300 °C (ethanol); ¹H NMR: 2.32 (s, 3H, CH₃), 3.74 (s, 3H, OCH₃), 6.94 (d, 2H, ar, *J* = 9.0 Hz), 7.60 (d, 2H, ar, *J* = 9.0), 10.25 (s, 1H, NH), 12.46 (br s, 1H, NH). IR: 3252, 1690. Anal. calc. for C₁₃H₁₂N₄O₂S.

5.1.12.3. 5-Methyl-2-((4-methylphenyl)amino)-thiazolo[5,4-*d*]pyrimidin-7-one **23**. Reaction time 60 min. Yield 88%; m.p. >300 °C (methanol); ¹H NMR: 2.27 (s, 3H, CH₃), 2.33 (s, 3H, CH₃), 7.16 (d, 2H, ar, *J* = 8.4 Hz), 7.59 (d, 2H, ar, *J* = 8.4 Hz), 10.35 (s, 1H, NH), 12.49 (br s, 1H, NH). IR: 3205, 1685, 1462. Anal. calc. for C₁₃H₁₂N₄O₂S.

5.1.12.4. 2-((4-Chlorophenyl)amino)-5-methyl-thiazolo[5,4-*d*]pyrimidin-7-one **24**. Reaction time 30 min. Yield 80%; m.p. >300 °C (methanol); ¹H NMR: 2.34 (s, 3H, CH₃), 7.41 (d, 2H, ar, *J* = 8.9 Hz),

7.75 (d, 2H, ar, *J* = 8.9 Hz), 10.60 (s, 1H, NH), 12.53 (br s, 1H, NH). IR: 3291, 3198, 1652. Anal. calc. for C₁₂H₉ClN₄O₂S.

5.1.12.5. 2-((3-Methoxyphenyl)amino)-5-methyl-thiazolo[5,4-*d*]pyrimidin-7-one **25**. Reaction time 23 h. Yield 85%; m.p. 286–287 °C (ethanol); ¹H NMR: 2.34 (s, 3H, CH₃), 3.76 (s, 3H, OCH₃), 6.61 (d, 1H, ar, *J* = 7.9 Hz), 7.19–7.27 (m, 2H, ar), 7.42 (s, 1H, ar), 10.45 (s, 1H, NH), 12.51 (br s, 1H, NH). ¹³C NMR: 160.32, 158.13, 155.88, 155.69, 154.36, 141.89, 134.06, 130.24, 110.54, 107.51, 104.33, 55.49, 21.25. IR: 3246, 3082, 1688. Anal. calc. for C₁₃H₁₂N₄O₂S.

5.1.12.6. 5-Methyl-2-((3-methylphenyl)amino)-thiazolo[5,4-*d*]pyrimidin-7-one **26**. Reaction time 28 h. Yield 91%; m.p. 290–291 °C (methanol); ¹H NMR: 2.31 (s, 3H, CH₃), 2.33 (s, 3H, CH₃), 6.84 (d, 1H, ar, *J* = 7.5 Hz), 7.23 (t, 1H, ar, *J* = 7.8 Hz), 7.46 (s, 1H, ar), 7.55 (d, 1H, ar, *J* = 7.8 Hz), 10.37 (s, 1H, NH), 12.51 (br s, 1H, NH). ¹³C NMR: 158.28, 155.88, 155.63, 154.26, 140.78, 138.69, 134.10, 129.33, 123.37, 118.45, 115.29, 21.78, 21.25. IR: 3196, 3143, 1686, 1463. Anal. calc. for C₁₃H₁₂N₄O₂S.

5.1.12.7. 2-((3-Chlorophenyl)amino)-5-methyl-thiazolo[5,4-*d*]pyrimidin-7-one **27**. Reaction time 30 min. Yield 93%; m.p. >300 °C (ethyl acetate); ¹H NMR: 2.34 (s, 3H, CH₃), 7.06 (d, 1H, ar, *J* = 7.9 Hz), 7.37 (t, 1H, ar, *J* = 8.0 Hz), 7.59 (d, 1H, ar, *J* = 8.0 Hz), 8.01 (s, 1H, ar), 10.67 (br s, 1H, NH), 12.57 (br s, 1H, NH). IR: 3271, 3187, 1673. Anal. calc. for C₁₂H₉ClN₄O₂S.

5.1.12.8. 2-((3,4-Dichlorophenyl)amino)-5-methyl-thiazolo[5,4-*d*]pyrimidin-7-one **28**. Reaction time 30 min. Yield 81%; m.p. >300 °C (ethanol); ¹H NMR: 2.34 (s, 3H, CH₃), 7.53–7.61 (m, 2H, ar), 8.18 (d, 1H, ar, *J* = 2.3 Hz), 10.79 (br s, 1H, NH), 12.60 (br s, 1H, NH). IR: 3203, 3148, 1664. Anal. calc. for C₁₂H₈Cl₂N₄O₂S.

5.1.13. General procedure for the synthesis of 2-aryl-7-chloro-5-methyl-thiazolo[5,4-*d*]pyrimidine derivatives (**76–78**)

A suspension of compounds **1**, **3**, **4** (5 mmol), *N,N*-dimethylaniline (1.15 mL) and POCl₃ (20 mL) was refluxed for 3 h. The solvent was evaporated under pressure, and the residue was added with brine (100 mL). The precipitate was collected and washed with water. The crude products were unstable upon recrystallization; however, they were pure enough to be used without further purification.

5.1.13.1. 7-Chloro-5-methyl-2-phenyl-thiazolo[5,4-*d*]pyrimidine **76**. Yield 92%; ¹H NMR: 2.75 (s, 3H, CH₃), 7.62–7.69 (m, 3H, ar), 8.15–8.16 (m, 2H, ar).

5.1.13.2. 7-Chloro-5-methyl-2-(4-methylphenyl)-thiazolo[5,4-*d*]pyrimidine **77**. Yield 94%; ¹H NMR: 2.40 (s, 3H, CH₃), 2.76 (s, 3H, CH₃), 7.45 (d, 2H, ar, *J* = 8.0 Hz), 8.04 (d, 2H, ar, *J* = 8.0 Hz).

5.1.13.3. 7-Chloro-2-(4-chlorophenyl)-5-methyl-thiazolo[5,4-*d*]pyrimidine **78**. Yield 94%; ¹H NMR: 2.76 (s, 3H, CH₃), 7.70 (d, 2H, ar, *J* = 8.6 Hz), 8.17 (d, 2H, ar, *J* = 8.6 Hz).

5.1.14. General procedure for the synthesis of 2-aryl-7-ethoxy-5-methyl-thiazolo[5,4-*d*]pyrimidine derivatives (**29–31**)

A suspension of compounds **76–78** (0.8 mmol), DBU (1.2 mmol) in absolute ethanol (8 mL) was microwave irradiated at 160 °C for 90 min. Evaporation of the solvent gives a solid which was collected, washed with diethyl ether and recrystallized.

5.1.14.1. 7-Ethoxy-5-methyl-2-phenyl-thiazolo[5,4-*d*]pyrimidine **29**. Yield 45%; m.p. 134–136 °C (ethanol); ¹H NMR: 1.46 (t, 3H, CH₃, *J* = 7.0 Hz), 2.65 (s, 3H, CH₃), 4.63 (q, 2H, CH₂, *J* = 7.0 Hz), 7.61 (m,

3H, ar), 8.08 (m, 2H, ar). Anal. calc. for C₁₄H₁₃N₃OS.

5.1.14.2. 7-Ethoxy-5-methyl-2-(4-methylphenyl)-thiazolo[5,4-d]pyrimidine **30**. Yield 68%; m.p. 146–149 °C (methanol); ¹H NMR: 1.45 (t, 3H, CH₃, *J* = 7.0 Hz), 2.40 (s, 3H, CH₃), 2.64 (s, 3H, CH₃), 4.62 (q, 2H, CH₂, *J* = 7.0 Hz), 7.40 (d, 2H, ar, *J* = 8.0 Hz), 7.97 (d, 2H, ar, *J* = 8.0 Hz). Anal. calc. for C₁₅H₁₅N₃O₂S.

5.1.14.3. 2-(4-Chlorophenyl)-7-ethoxy-5-methyl-thiazolo[5,4-d]pyrimidine **31**. Yield 56%; m.p. 148–150 °C (ethanol); ¹H NMR: 1.46 (t, 3H, CH₃, *J* = 7.0 Hz), 2.64 (s, 3H, CH₃), 4.61 (q, 2H, CH₂, *J* = 7.0 Hz), 7.65 (d, 2H, ar, *J* = 8.5 Hz), 8.10 (d, 2H, ar, *J* = 8.5 Hz). Anal. calc. for C₁₄H₁₂ClN₃O₂S.

5.1.15. 7-Ethoxy-5-methyl-N-phenyl-thiazolo[5,4-d]pyrimidin-2-amine **32**

A solution of the 7-chloro derivative **68** (0.6 mmol) in ethanol (10 mL) was treated with an aqueous solution of NaOH (20%, 20 mL). The mixture was refluxed for 5 h, then cooled to room temperature. Addition of H₂O afforded a precipitate which was collected, washed with water and recrystallised. Yield 43%; m.p. 105–106 °C (ethanol); ¹H NMR: 1.41 (t, 3H, CH₃, *J* = 7.0 Hz), 2.54 (s, 3H, CH₃), 4.55 (q, 2H, CH₂, *J* = 7.0 Hz), 7.06 (t, 1H, ar, *J* = 7.1 Hz), 7.39 (t, 2H, ar, *J* = 7.4 Hz), 7.72 (d, 2H, ar, *J* = 7.8 Hz), 10.67 (br s, 1H, NH). Anal. calc. for C₁₄H₁₄N₄O₂S.

5.1.16. 7-Ethoxy-N-(3-methoxyphenyl)-5-methyl-thiazolo[5,4-d]pyrimidin-2-amine **33**

Sodium ethoxide (2.4 mmol) was added to a solution of the 7-chloro derivative **72** (1.2 mmol) in absolute ethanol (5 mL). The reaction mixture was refluxed, under nitrogen atmosphere, for 7 h and then cooled to room temperature. The precipitate was collected by filtration, resuspended in H₂O (5 mL), and acidified to pH 4–5 with acetic acid. The solid was collected, washed with water and recrystallised. Yield 63%; m.p. 150–151 °C (ethanol); ¹H NMR: 1.40 (t, 3H, CH₃, *J* = 7.1 Hz), 2.54 (s, 3H, CH₃), 3.78 (s, 3H, OCH₃), 4.54 (q, 2H, CH₂, *J* = 7.1 Hz), 6.65 (dd, 1H, ar, *J* = 8.1, 1.8 Hz), 7.21 (dd, 1H, ar, *J* = 8.1, 1.8 Hz), 7.29 (t, 1H, ar, *J* = 8.1 Hz), 7.47 (s, 1H, ar), 10.67 (s, 1H, NH). ¹³C NMR: 161.47, 160.36, 160.30, 158.84, 158.10, 141.63, 130.33, 129.18, 110.88, 108.18, 104.63, 62.62, 55.43, 25.67, 14.86. Anal. calc. for C₁₅H₁₆N₄O₂S.

5.2. Molecular modeling studies

5.2.1. Computational methodologies

All molecular modeling studies were performed on a 2 CPU (PIV 2.0–3.0 GHz) Linux PC. Homology modeling, energy minimization, and docking studies were carried out using Molecular Operating Environment (MOE, version 2010.10) suite [44]. Manual docking and Monte Carlo studies of the MRS 1220 binding mode were done using MOE and Schrodinger MacroModel (ver. 8.0) [46] with Schrodinger Maestro interface. Compounds docking analyses were then performed with MOE. All ligand structures were optimized using RHF/AM1 semiempirical calculations and the software package MOPAC [47] implemented in MOE was utilized for these calculations.

5.2.2. Homology modeling of the human A₃AR

The homology model of the hA₃AR was built using the X-ray structure of the antagonist-bound hA_{2A}AR as template (pdb code: 3EML; 2.6 Å resolution [42]). A multiple alignment of the AR primary sequences was built within MOE as preliminary step. The sequence alignment of the four human ARs is shown within [Supplementary data](#). The boundaries identified from the used X-ray crystal structure of hA_{2A}AR were then applied for the

corresponding sequences of the TM helices of the hA₃AR. The missing loop domains were built by the loop search method implemented in MOE. Once the heavy atoms were modeled, all hydrogen atoms were added, and the protein coordinates were then minimized with MOE using the AMBER99 [52] force field. The minimizations were performed by steepest descent steps followed by conjugate gradient minimization until the RMS gradient of the potential energy was less than 0.05 kJ mol⁻¹ Å⁻¹. Reliability and quality of the model was checked using the Protein Geometry Monitor application within MOE, which provides a variety of stereochemical measurements for inspection of the structural quality in a given protein, like backbone bond lengths, angles and dihedrals, Ramachandran φ-ψ dihedral plots, and sidechain rotamer and nonbonded contact quality.

5.2.3. Preliminary analysis with MRS 1220

A preliminary docking analysis was performed by manually docking MRS 1220 structure within the hA₃AR model binding site. The obtained hA₃AR-MRS 1220 complex was then subjected to energy minimization refinement and to Monte Carlo analysis to explore the favorable binding conformations. This analysis was conducted by Monte Carlo Conformational Search protocol implemented in Schrodinger MacroModel. The input structure consisted of the ligand and a shell of receptor amino acids within the specified distance (6 Å) from the ligand. The coordinates of the remaining receptor residues were kept fixed. During the Monte Carlo conformational searching, the input structure was modified by random changes in user-specified torsion angles (for all input structure residues), and molecular position (for the ligand). Hence, the ligand was left free to be continuously re-oriented within the binding site and the conformation of both ligand and internal shell residues could be explored and reciprocally relaxed. The method consisted of 10,000 Conformational Search steps with MMFF94s [53–59] force field. The best hA₃AR-MRS 1220 complex was saved and subjected to energy minimization with the same protocol as above. This protocol was recently used to prepare hA₃AR models for docking and dynamics studies of nucleoside agonists at the same receptor [50,60].

5.2.4. Molecular docking analysis

All compound structures were docked into the binding site of the hA₃AR model using the MOE Dock tool. This method is divided into a number of stages: *Conformational Analysis of ligands*. The algorithm generated conformations from a single 3D conformation by conducting a systematic search. In this way, all combinations of angles were created for each ligand. *Placement*. A collection of poses was generated from the pool of ligand conformations using Triangle Matcher placement method. Poses were generated by superposition of ligand atom triplets and triplet points in the receptor binding site. The receptor site points are alpha sphere centers which represent locations of tight packing. At each iteration a random conformation was selected, a random triplet of ligand atoms and a random triplet of alpha sphere centers were used to determine the pose. *Scoring*. Poses generated by the placement methodology were scored using two available methods implemented in MOE, the *London dG* scoring function which estimates the free energy of binding of the ligand from a given pose, and *Affinity dG* scoring which estimates the enthalpic contribution to the free energy of binding. The top 30 poses for each ligand were output in a MOE database.

5.2.5. Post docking analysis

The five top-score docking poses of each compound were then subjected to AMBER99 force field energy minimization until the RMS gradient of the potential energy was less than

0.05 kJ mol⁻¹ Å⁻¹. Receptor residues within 6 Å distance from the ligand were left free to move, while the remaining receptor coordinates were kept fixed. AMBER99 partial charges of receptor and MOPAC output partial charges of ligands were utilized. Once the compound-binding site energy minimization was completed, receptor coordinates were fixed and a second energy minimization stage was performed leaving free to move only compound atoms. MMFF94 force field was applied. For each compound, the minimized docking poses were then rescored using *London dG* and *Afinity dG* scoring functions and the *dock-pK_i* predictor. The latter tool allows estimating the pK_i for each ligand using the “scoring.svl” script retrievable at the SVL exchange service (Chemical Computing Group, Inc. SVL exchange: <http://svl.chemcomp.com>). The algorithm is based on an empirical scoring function consisting of a directional hydrogen-bonding term, a directional hydrophobic interaction term, and an entropic term (ligand rotatable bonds immobilized in binding). For each compound, the top-score docking poses according to at least two out of three scoring functions were selected for final ligand–target interaction analysis. The interactions between the ligands **25** and **33** and the receptors binding site were analyzed by using the *IF-E 6.0* tool [49] retrievable at the SVL exchange service. The program calculates and displays the atomic and residue interaction forces as 3D vectors. It also calculates the per-residue interaction energies, where negative and positive energy values (expressed as kcal mol⁻¹) are associated to favorable and unfavorable interactions, respectively. A shell of residues contained within a 10 Å distance from ligand were considered for this analysis.

5.3. Pharmacology

5.3.1. Human cloned A₁, A_{2A}, and A₃AR receptor binding assay

All synthesized compounds were tested to evaluate their affinity to hA₁, hA_{2A} and hA₃ARs stably expressed in CHO cells. The cells were grown adherently and maintained in Dulbecco's modified Eagles medium with nutrient mixture F12 (DMEM/F12) without nucleosides, containing 10% fetal calf serum, penicillin (100 U/mL), streptomycin (100 µg/mL), L-glutamine (2 mM) and Geneticin (G418, 0.2 mg/mL) at 37 °C in 5% CO₂, 95% air. For membrane preparation the culture medium was removed and the cells were washed with PBS and scraped off T75 flasks in ice-cold hypotonic buffer (5 mM Tris HCl, 2 mM EDTA, pH 7.4). The cell suspension was homogenized with Polytron and the homogenate was spun for 10 min at 1000×g. The supernatant was then centrifuged for 30 min at 100,000×g [28]. The membrane pellet was suspended in: a) 50 mM Tris HCl buffer pH 7.4 for A₁ARs; b) 50 mM Tris HCl, 10 mM MgCl₂ buffer pH 7.4 for A_{2A}ARs; c) 50 mM Tris HCl, 10 mM MgCl₂, 1 mM EDTA buffer pH 7.4 for A₃ARs. The cell suspension was incubated with 2 IU/mL of adenosine deaminase for 30 min at 37 °C. The membrane preparation was used to perform binding experiments. Displacement experiments of [³H] DPCPX (1 nM) to hA₁ CHO membranes (50 µg of protein/assay) and at least six to eight different concentrations of the compounds for 120 min at 25 °C in 50 mM Tris HCl buffer pH 7.4 were performed [30]. Non-specific binding was determined in the presence of 1 µM of DPCPX (≤10% of the total binding). Binding of [³H] ZM-241385 (1 nM) to hA_{2A}CHO membranes (50 µg of protein/assay) was performed using 50 mM Tris HCl buffer, 10 mM MgCl₂ pH 7.4 and at least six to eight different concentrations of antagonists studied for an incubation time of 60 min at 4 °C [30]. Non-specific binding was determined in the presence of 1 µM ZM 241385 and was about 20% of total binding. Competition binding experiments to hA₃CHO membranes (50 µg of protein/assay) and 0.5 nM [¹²⁵I]AB-MECA, 50 mM Tris HCl buffer, 10 mM MgCl₂, 1 mM EDTA, pH 7.4 and at least six to eight different concentrations of

examined ligands for 120 min at 4 °C [61]. Non-specific binding was defined as binding in the presence of 1 µM AB-MECA and was about 20% of total binding. Bound and free radioactivity were separated by filtering the assay mixture through Whatman GF/B glass fiber filters using a Brandel cell harvester. The filter bound radioactivity was counted by Scintillation Counter Packard Tri Carb 2810 TR with an efficiency of 62%.

5.3.2. Measurement of cyclic AMP levels in CHO cells transfected with hA_{2B} or hA₃ARs

CHO cells transfected with hAR subtypes were washed with phosphate-buffered saline, diluted trypsin and centrifuged for 10 min at 200g. The cells (1 × 10⁶ cells/assay) were suspended in 0.5 mL of incubation mixture (mM): NaCl 15, KCl 0.27, NaH₂PO₄ 0.037, MgSO₄ 0.1, CaCl₂ 0.1, Hepes 0.01, MgCl₂ 1, glucose 0.5, pH 7.4 at 37 °C, 2 IU/mL adenosine deaminase, and 4-(3-butoxy-4-methoxybenzyl)-2-imidazolidinone (Ro 20–1724) as phosphodiesterase inhibitor and preincubated for 10 min in a shaking bath at 37 °C. The potency of antagonists to hA_{2B}AR was determined by the inhibition of NECA (200 nM)-induced cyclic AMP production [62]. In addition, the potency of antagonists to hA₃ARs was determined in the presence of forskolin 1 µM and Cl-IB-MECA (100 nM) that mediated inhibition of cyclic AMP levels [61]. The reaction was terminated by the addition of cold 6% trichloroacetic acid (TCA). The TCA suspension was centrifuged at 2000g for 10 min at 4 °C, and the supernatant was extracted four times with water saturated diethyl ether. The final aqueous solution was tested for cyclic AMP levels by a competition protein binding assay. Samples of cyclic AMP standard (0–10 pmol) were added to each test tube containing [³H] cAMP and incubation buffer (trizma base 0.1 M, aminophylline 8.0 mM, 2-mercaptoethanol 6.0 mM, pH 7.4). The binding protein prepared from beef adrenals was added to the samples previously incubated at 4 °C for 150 min, and, after the addition of charcoal, was centrifuged at 2000g for 10 min. The clear supernatant was counted in a Scintillation Counter Packard Tri Carb 2810 TR with an efficiency of 58%.

5.3.3. Data analysis

The protein concentration was determined according to a Bio-Rad method with bovine albumin as a standard reference [61]. Inhibitory binding constant (K_i) values were calculated from those of IC₅₀ according to Cheng & Prusoff equation $K_i = IC_{50} / (1 + [C^*] / K_D^*)$, where [C*] is the concentration of the radioligand and K_D* its dissociation constant [61]. A weighted non linear least-squares curve fitting program LIGAND was used for computer analysis of inhibition experiments [61]. IC₅₀ values obtained in cyclic AMP assay were calculated by nonlinear regression analysis using the equation for a sigmoid concentration–response curve (Graph-PAD Prism, San Diego, CA, U.S.A) [61,62].

Acknowledgments

The synthetic work was financially supported by the University of Florence, the Italian Ministry for University and Research (MIUR, PRIN 2010–2011, 20103779_04 project) and the Ente Cassa di Risparmio di Firenze (2013.0664A2202.3926 project). The molecular modeling work has been carried out with financial support from the University of Camerino, Italy, and the Italian Ministry for University and Research, Rome, Italy.

Appendix A. Supplementary data

Supplementary data related to this article can be found at <http://dx.doi.org/10.1016/j.ejmech.2015.04.010>.

References

- [1] B.B. Fredholm, A.P. Ijzerman, K.A. Jacobson, K.-N. Klotz, J. Linden, International union of pharmacology XXV. Nomenclature and classification of adenosine receptors, *Pharmacol. Rev.* 53 (2001) 527–552.
- [2] B.B. Fredholm, A.P. Ijzerman, K.A. Jacobson, J. Linden, C.E. Muller, International union of pharmacology LXXXI. Nomenclature and classification of adenosine receptors. An up date, *Pharmacol. Rev.* 63 (2011) 1–34.
- [3] B.B. Fredholm, R.A. Cunha, P. Svenningsson, Pharmacology of adenosine receptors and therapeutic applications, *Curr. Top. Med. Chem.* 3 (2002) 413–426.
- [4] K.A. Jacobson, Z.-G. Gao, Adenosine receptors as therapeutic targets, *Nat. Rev. Drug Discov.* 5 (2006) 247–264.
- [5] G. Hasko, J. Linden, B. Cronstein, P. Pacher, Adenosine receptors: therapeutic aspects for inflammatory and immune diseases, *Nat. Rev. Drug Discov.* 7 (2008) 759–770.
- [6] C.E. Muller, K.A. Jacobson, Recent developments in adenosine receptor ligands and their potential as novel drugs, *Biochim. Biophys. Acta* 1808 (2011) 1290–1308.
- [7] S.L. Cheong, S. Federico, G. Venkatesan, A.L. Mandel, Y.-M. Shao, S. Moro, G. Spalluto, G. Pastorin, The A₃ adenosine receptor as multifaceted therapeutic target: pharmacology, medicinal chemistry and in silico approaches, *Med. Chem. Rev.* 33 (2013) 235–335.
- [8] A.M. Pugliese, E. Coppi, R. Volpini, G. Cristalli, R. Corradetti, L.S. Jeong, K.A. Jacobson, F. Pedata, Role of adenosine A₃ receptors on CA1 hippocampal neurotransmission during oxygenglucose deprivation episodes of different duration, *Biochem. Pharmacol.* 74 (2007) 768–779.
- [9] S. Merighi, A. Benini, P. Mirandola, S. Gessi, K. Varani, E. Leung, S. MacLennan, P.A. Borea, Adenosine modulates vascular endothelial growth factor expression via hypoxia-inducible factor-1 in human glioblastoma cells, *Biochem. Pharmacol.* 72 (2006) 19–31.
- [10] S. Gessi, E. Cattabriga, A. Avitabile, R. Gafa', G. Lanza, L. Cavazzini, N. Bianchi, R. Gambari, C. Feo, A. Liboni, S. Gullini, E. Leung, S. MacLennan, P.A. Borea, Elevated expression of A₃ adenosine receptors in human colorectal cancer is reflected in peripheral blood cells, *Clin. Cancer Res.* 10 (2004) 5895–5901.
- [11] S. Gessi, S. Merighi, K. Varani, E. Leung, S. MacLennan, P.A. Borea, The A₃ adenosine receptor: an enigmatic player in cell biology, *Pharmacol. Ther.* 117 (2008) 123–140.
- [12] D. Boison, J.-F. Chen, B.B. Fredholm, Adenosine signaling and function in glial cells, *Cell Death Differ.* 17 (2010) 1071–1082.
- [13] W. Liu, Y. Tang, J. Feung, Cross talk between activation of microglia and astrocytes in pathological conditions in the central nervous system, *Life Sci.* 89 (2011) 141–146.
- [14] Z. Chen, K. Janes, C. Chen, T. Doyle, L. Bryant, D.K. Tosh, K.A. Jacobson, D. Salvemini, Controlling murine and rat chronic pain through A₃ adenosine receptor activation, *FASEB J.* 26 (2012) 1855–1865.
- [15] V. Colotta, D. Catarzi, F. Varano, L. Cecchi, G. Filacchioni, C. Martini, L. Trincavelli, A. Lucacchini, 1,2,4-Triazolo[4,3-a]quinoxalin-1-one: a versatile tool for the synthesis of potent and selective adenosine receptor antagonists, *J. Med. Chem.* 43 (2000) 1158–1164.
- [16] V. Colotta, D. Catarzi, F. Varano, L. Cecchi, G. Filacchioni, C. Martini, L. Trincavelli, A. Lucacchini, Synthesis and structure-activity relationships of a new set of 2-aryl-pyrazolo[3,4-c]quinoline derivatives as adenosine receptor antagonists, *J. Med. Chem.* 43 (2000) 3118–3124.
- [17] V. Colotta, D. Catarzi, F. Varano, F.R. Calabri, O. Lenzi, G. Filacchioni, C. Martini, L. Trincavelli, F. Deflorian, S. Moro, The 1,2,4-Triazolo[4,3-a]quinoxalin-1-one moiety as an attractive scaffold to develop new potent and selective human A₃ adenosine receptor antagonists: synthesis, pharmacological and ligand-receptor modeling studies, *J. Med. Chem.* 47 (2004) 3580–3590.
- [18] D. Catarzi, V. Colotta, F. Varano, O. Lenzi, G. Filacchioni, L. Trincavelli, C. Martini, C. Montopoli, S. Moro, 1,2,4-Triazolo[1,5-a]quinoxaline as a versatile tool for the design human A₃ adenosine receptor antagonists: synthesis, biological evaluation, and molecular modelling studies of 2-(hetero)aryl- and 2-carboxy-substituted derivatives, *J. Med. Chem.* 48 (2005) 7932–7945.
- [19] O. Lenzi, V. Colotta, D. Catarzi, F. Varano, G. Filacchioni, C. Martini, L. Trincavelli, O. Ciampi, K. Varani, F. Marighetti, E. Morizzo, S. Moro, 4-Amido-2-aryl-1,2,4-triazolo[4,3-a]quinoxalin-1-ones as new potent and selective human A₃ adenosine receptor antagonists: synthesis, pharmacological evaluation, and ligand-receptor modelling studies, *J. Med. Chem.* 49 (2006) 3916–3925.
- [20] V. Colotta, D. Catarzi, F. Varano, F. Capelli, O. Lenzi, G. Filacchioni, C. Martini, L. Trincavelli, O. Ciampi, A.M. Pugliese, F. Pedata, A. Schiesaro, E. Morizzo, S. Moro, New 2-arylpyrazolo[3,4-c]quinoline derivatives as potent and selective human A₃ adenosine receptor antagonists. Synthesis, pharmacological evaluation and ligand-receptor modeling studies, *J. Med. Chem.* 50 (2007) 4061–4074.
- [21] E. Morizzo, F. Capelli, O. Lenzi, D. Catarzi, F. Varano, G. Filacchioni, F. Vincenzi, K. Varani, P.A. Borea, V. Colotta, S. Moro, Scouting human A₃ adenosine receptor antagonist binding mode using a molecular simplification approach: from triazoliquinoxaline to a pyrimidine skeleton as a key study, *J. Med. Chem.* 50 (2007) 6596–6606.
- [22] V. Colotta, D. Catarzi, F. Varano, O. Lenzi, G. Filacchioni, C. Martini, L. Trincavelli, O. Ciampi, C. Traini, A.M. Pugliese, F. Pedata, E. Morizzo, S. Moro, Synthesis, ligand-receptor modeling studies and pharmacological evaluation of novel 4-modified-2-aryl-1,2,4-triazolo[4,3-a]quinoxalin-1-one derivatives as potent and selective human A₃ adenosine receptor antagonists, *Bioorg. Med. Chem.* 16 (2008) 6086–6102.
- [23] O. Lenzi, V. Colotta, D. Catarzi, F. Varano, D. Poli, G. Filacchioni, K. Varani, F. Vincenzi, P.A. Borea, S. Paoletta, E. Morizzo, S. Moro, 2-Phenylpyrazolo[4,3-d]pyrimidin-7-one as a new scaffold to obtain potent and selective human A₃ adenosine receptor antagonists: new insights into the receptor-antagonist recognition, *J. Med. Chem.* 52 (2009) 7640–7652.
- [24] V. Colotta, O. Lenzi, D. Catarzi, F. Varano, G. Filacchioni, C. Martini, L. Trincavelli, O. Ciampi, A.M. Pugliese, C. Traini, F. Pedata, E. Morizzo, S. Moro, Pyrido[2,3-e]-1,2,4-triazolo[4,3-a]pyrazin-1-one as a new scaffold to develop potent and selective human A₃ adenosine receptor antagonists. Synthesis, pharmacological evaluation, and ligand-receptor modeling studies, *J. Med. Chem.* 52 (2009) 2407–2419.
- [25] V. Colotta, F. Capelli, O. Lenzi, D. Catarzi, F. Varano, D. Poli, F. Vincenzi, K. Varani, P.A. Borea, D. Dal Ben, R. Volpini, G. Cristalli, G. Filacchioni, Novel potent and highly selective human A₃ adenosine receptor antagonists belonging to the 4-amido-2-arylpyrazolo[3,4-c]quinoline series: molecular docking analysis and pharmacological studies, *Bioorg. Med. Chem.* 17 (2009) 401–410.
- [26] D. Poli, D. Catarzi, V. Colotta, F. Varano, G. Filacchioni, S. Daniele, L. Trincavelli, C. Martini, S. Paoletta, S. Moro, The identification of the 2-phenylphthalazin-1(2H)-one scaffold as a new decorable core skeleton for the design of potent and selective human A₃ adenosine receptor antagonists, *J. Med. Chem.* 54 (2011) 2102–2113.
- [27] O. Lenzi, V. Colotta, D. Catarzi, F. Varano, L. Squarcialupi, G. Filacchioni, K. Varani, F. Vincenzi, P.A. Borea, D. Dal Ben, C. Lambertucci, G. Cristalli, Synthesis, structure-affinity relationships, and molecular modeling studies of novel pyrazolo[3,4-c]quinoline derivatives as adenosine receptor antagonists, *Bioorg. Med. Chem.* 19 (2011) 3757–3768.
- [28] L. Squarcialupi, V. Colotta, D. Catarzi, F. Varano, G. Filacchioni, K. Varani, C. Corciulo, F. Vincenzi, P.A. Borea, C. Ghelardini, L. Di Cesare Mannelli, A. Ciancetta, S. Moro, 2-Arylpyrazolo[4,3-d]pyrimidin-7-amino derivatives as new potent and selective human A₃ adenosine receptor antagonists. Molecular modeling studies and pharmacological evaluation, *J. Med. Chem.* 56 (2013) 2256–2269.
- [29] D. Catarzi, V. Colotta, F. Varano, D. Poli, L. Squarcialupi, G. Filacchioni, K. Varani, F. Vincenzi, P.A. Borea, D. Dal Ben, C. Lambertucci, G. Cristalli, Pyrazolo[1,5-c]quinazoline derivatives and their simplified analogues as adenosine receptor antagonists: synthesis, structure-affinity relationships and molecular modeling studies, *Bioorg. Med. Chem.* 21 (2013) 283–294.
- [30] L. Squarcialupi, V. Colotta, D. Catarzi, F. Varano, M. Betti, K. Varani, F. Vincenzi, P.A. Borea, N. Porta, A. Ciancetta, S. Moro, 7-Amino-2-phenylpyrazolo[4,3-d]pyrimidine derivatives: structural investigations at the 5-position to target human A₁ and A_{2A} adenosine receptors. Molecular modeling and pharmacological studies, *Eur. J. Med. Chem.* 84 (2014) 614–627.
- [31] T. Seitz, J. Baudoux, H. Bekolo, D. Cahard, J.-C. Plaquevent, M.-C. Lasneand, J. Rouden, Organocatalyzed route to enantioenriched pipercol esters: decarboxylation of an aminomalonate hemiester, *Tetrahedron* 62 (2006) 6155–6165.
- [32] Daiichi Pharmaceutical, Five membered heterocyclic derivatives. EP 1621537A1 2006.
- [33] Lee Byoung-Suk, Chun Myung-Hee, Process for preparing 2-(4-chlorobenzoylamino)-3[(1H)-quinolinon-4yl]propionic acid, US 2003/87930A1 2003.
- [34] M.-Y. Jang, Y. Lin, S. De Jonghe, L.-J. Gao, B. Vanderhoydonck, M. Froeyen, J. Rozenski, J. Herman, T. Louat, K. Van Belle, M. Waer, P. Herdewijn, Discovery of 7-N-Piperazinylthiazolo[5,4-d]pyrimidine analogues as a novel class of immunosuppressive agents with in vivo biological activity, *J. Med. Chem.* 54 (2011) 655–668.
- [35] Sanofi, D. Kadereit, M. Schaefer, S. Hachtel, A. Dietrich, T. Huebschle, A. Gille, K. Hiss, 2,5,7-Substituted-oxazolopyrimidines derivatives, US 2013/137685A1 2013.
- [36] Sanofi, D. Kadereit, M. Schaefer, W. Czechtisky. WO 2010/6704A1 2010.
- [37] S.V. Ley, A. Priour, Total synthesis of the cyclic peptide argyirin, *Eur. J. Org. Chem.* (2002) 3995–4004.
- [38] V.V. Narayanan, S.R. Gopalan, D. Srinivasa, S.M. Mobin, P. Mathur, Crystal structure and energy optimization of dichlorobis(ethylthranilatonicotinamide) Zinc (II), *J. Chem. Cryst.* 41 (2011) 801–805.
- [39] Riberau, Queguiner, Synthesis and physical properties of the six furylpyridines, *Can. J. Chem.* 61 (1983) 334–342.
- [40] Katholieke Universiteit Leuven, K. V. Leuven Rand, J. Herman, T. Louat, Anticancer activity of novel bicyclic heterocycles, US2014/88088A1 2014.
- [41] S. Ye-Xiang, D. Ya-Hui, M. Ting-Ting, L. Yu-Yan, S. Li-Ping, "On water" direct Pd-catalyzed C-H arylation of thiazolo[5,4-d]pyrimidine derivatives, *Green Chem.* 14 (2012) 1979–1981.
- [42] V.P. Jaakola, M.T. Griffith, M.A. Hanson, V. Cherezov, E.Y. Chien, J.R. Lane, A.P. Ijzerman, R.C. Stevens, The 2.6 angstrom crystal structure of a human A_{2A} adenosine receptor bound to an antagonist, *Science* 322 (2008) 1211.
- [43] D. Dal Ben, C. Lambertucci, G. Marucci, R. Volpini, G. Cristalli, Adenosine receptor modeling: what does the A_{2A} crystal structure tell us? *Curr. Top. Med. Chem.* 10 (2010) 993–1018.
- [44] Molecular Operating Environment; C.C.G., Inc., 1255 University St., Suite 1600, Montreal, Quebec, Canada, H3B 3X3.
- [45] Y.C. Kim, X.D. Ji, K.A. Jacobson, Derivatives of the triazoloquinazoline

- adenosine antagonist (CGS15943) are selective for the human A_3 receptor subtype, *J. Med. Chem.* 39 (1996) 4142–4148.
- [46] F. Mohamadi, N.G.J. Richards, W.C. Guida, R. Liskamp, M. Lipton, C. Caufield, G. Chang, T. Hendrickson, W.C. Still, MacroModel – an integrated software system for modeling organic and bioorganic molecules using molecular mechanics, *J. Comput. Chem.* 11 (1990) 440–467.
- [47] J.J. Stewart, MOPAC: a semiempirical molecular orbital program, *J. Comput. Aided Mol. Des.* 4 (1990) 1–105.
- [48] J.A. Ballesteros, H. Weinstein, Integrated methods for the construction of three-dimensional models and computational probing of structure–function relations in G protein-coupled receptors, *Methods Neurosci.* 25 (1995) 366–428.
- [49] H. Shadnia, J.S. Wright, J.M. Anderson, Interaction force diagrams: new insight into ligand–receptor binding, *J. Comput. Aided Mol. Des.* 23 (2009) 185–194.
- [50] D. Dal Ben, M. Buccioni, C. Lambertucci, G. Marucci, A. Thomas, R. Volpini, G. Cristalli, Molecular modelling study on potent and selective adenosine A_3 receptor agonists, *Bioorg. Med. Chem.* 18 (2010) 7923–7930.
- [51] D. Dal Ben, M. Buccioni, C. Lambertucci, A. Thomas, R. Volpini, Simulation and comparative analysis of binding modes of nucleoside and non-nucleoside agonists at the A_{2B} adenosine receptor, *Silico Pharmacol.* 1 (2013) 24.
- [52] W.D. Cornell, P. Cieplak, C.I. Bayly, I.R. Gould, K.M. Merz, D.M. Ferguson, D.C. Spellmeyer, T. Fox, J.W. Caldwell, P.A. Kollman, A second generation force field for the simulation of proteins, nucleic acids, and organic molecules, *J. Am. Chem. Soc.* 117 (1995) 5179–5197.
- [53] T.A. Halgren, Merck molecular force field. I. Basis, form, scope, parameterization, and performance of MMFF94, *J. Comput. Chem.* 17 (1996) 490–519.
- [54] T.A. Halgren, Merck Molecular Force Field. II. MMFF94 van der Waals and Electrostatic Parameters for Intermolecular Interactions, *J. Comput. Chem.* 17 (1996) 520–552.
- [55] T.A. Halgren, Merck molecular force field. III. Molecular geometries and vibrational frequencies for MMFF94, *J. Comput. Chem.* 17 (1996) 553–586.
- [56] T.A. Halgren, Merck molecular force field. IV. Conformational energies and geometries for MMFF94, *J. Comput. Chem.* 17 (1996) 587–615.
- [57] T.A. Halgren, R. Nachbar, Merck molecular force field. V. Extension of MMFF94 using experimental data, additional computational data, and empirical rules, *J. Comput. Chem.* 17 (1996) 616–641.
- [58] T.A. Halgren, MMFF VI. MMFF94s option for energy minimization studies, *J. Comput. Chem.* 20 (1999) 720–729.
- [59] T.A. Halgren, MMFF VII. Characterization of MMFF94, MMFF94s, and other widely available force fields for conformational energies and for intermolecular–interaction energies and geometries, *J. Comput. Chem.* 20 (1999) 730–748.
- [60] D. Dal Ben, M. Buccioni, C. Lambertucci, S. Kachler, N. Falgner, G. Marucci, A. Thomas, G. Cristalli, R. Volpini, K.-N. Klotz, Different efficacy of adenosine and NECA derivatives at the human A_3 adenosine receptor: insight into the receptor activation switch, *Biochem. Pharmacol.* 87 (2014) 321–331.
- [61] K. Varani, S. Merighi, S. Gessi, K.N. Klotz, E. Leung, P.G. Baraldi, B. Cacciari, R. Romagnoli, G. Spalluto, P.A. Borea, [3 H]-MRE 3008-F20: a novel antagonist radioligand for the pharmacological and biochemical characterization of human A_3 adenosine receptors, *Mol. Pharmacol.* 57 (2000) 968–975.
- [62] K. Varani, S. Gessi, S. Merighi, F. Vincenzi, E. Cattabriga, A. Benini, K.-N. Klotz, P.G. Baraldi, M.-A. Tabrizi, S. Mac Lennan, E. Leung, P.A. Borea, Pharmacological characterization of novel adenosine ligands in recombinant and native human A_{2B} receptors, *Biochem. Pharmacol.* 70 (2005) 1601–1612.